https://ntrs.nasa.gov/search.jsp?R=19780025933 2020-03-22T01:47:15+00:00Z

PROPAGATION OF SOUND THROUGH A SHEARED FLOW

by

James P. Woolley
Charles A. Smith
Krishnamurty Karamcheti

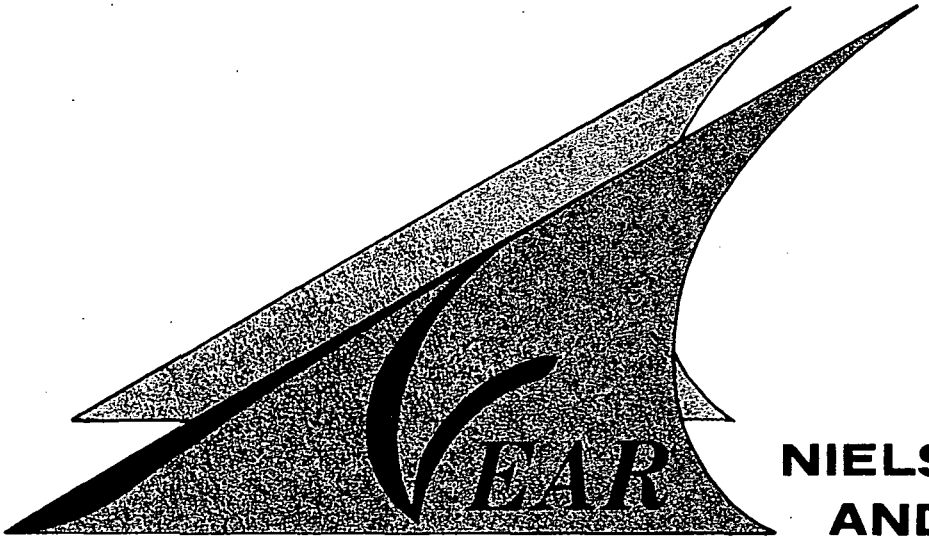

NIELSEN ENGINEERING
AND RESEARCH, INC.

OFFICES: 510 CLYDE AVENUE / MOUNTAIN VIEW, CALIFORNIA 94043 / TELEPHONE (415) 968-9457

PROPAGATION OF SOUND THROUGH A SHEARED FLOW

by

James P. Woolley
Charles A. Smith
Krishnamurty Karamcheti

NEAR TR 171

September 1979

Prepared under Contract No. NAS2-9357

by

NIELSEN ENGINEERING & RESEARCH, INC.
Mountain View, California 94043

for

NATIONAL AERONAUTICS AND SPACE ADMINISTRATION
Ames Research Center
Moffett Field, California 94035

COPY NO. 2

1. Report No.	2. Government Accession No.	3. Recipient's Catalog No.
NASA CR-152299		

4. Title and Subtitle	5. Report Date
PROPAGATION OF SOUND THROUGH A SHEARED FLOW	September 1979
	6. Performing Organization Code: 339/C

7. Author(s)	8. Performing Organization Report No.
J. P. Woolley, C. A. Smith, and K. Karamcheti	NEAR TR 171
	10. Work Unit No.

9. Performing Organization Name and Address	11. Contract or Grant No.
Nielsen Engineering & Research, Inc. 510 Clyde Avenue Mountain View, California 94043	NAS2-9357
	13. Type of Report and Period Covered: final report 8/30/76-7/1/77

12. Sponsoring Agency Name and Address	14. Sponsoring Agency Code
National Aeronautics and Space Administration Ames Research Center Moffett Field, California 94035	

15. Supplementary Notes

16. Abstract

Sound generated in a moving fluid must propagate through a shear layer in order to be measured by a fixed instrument, whether the microphone is placed in or outside of the flow. Passage through such a shear layer can significantly alter the features of the sound. These alterations must be accounted for if one wishes to characterize the nature of the sound sources from such measurements. The present investigation was initiated to provide means of evaluating and correcting for these propagation effects for noise sources typically associated with single and co-flowing subsonic jets and for subcritical flow over airfoils in such jets.

The techniques for describing acoustic propagation fall into two categories; geometric acoustics and wave acoustics. Geometric acoustics has much in common with geometric optics and is most convenient and accurate for high frequency sound. Wave acoustics is generally applicable to sound of all frequencies but is computationally difficult, and valid formulations, much less solutions, are known for only very restricted types of flows.

In the frequency range of interest to the present study (greater than 150 Hz), the geometric acoustics approach was determined to be the most useful and practical (continued next page)

17. Key Words (Suggested by Author(s))	18. Distribution Statement
sound propagation shear flow geometric acoustics jet noise	Unlimited

19. Security Classif. (of this report)	20. Security Classif. (of this page)	21. No. of Pages	22. Price*
Unclassified	Unclassified	83	

*For sale by the National Technical Information Service, Springfield, Virginia 22161

16. Abstract (continued)

method for describing the passage of sound through jets. Calculation methods and a computer program were developed to aid in the interpretation of results. This report describes these results, together with some background information on the general nature of sound propagation through shear layers.

TABLE OF CONTENTS

Section	Page
SUMMARY	1
INTRODUCTION	2
NOMENCLATURE	3
NATURE OF PROBLEM	5
BACKGROUND	7
Theory	7
Experiment	11
THEORETICAL BASIS OF GEOMETRIC ACOUSTICS	12
Kinematics of Wave Propagation in a Three-Dimensional, Inhomogeneous, Moving Medium	12
The Variational Problem and Its Solution	15
SOUND PROPAGATION IN A STRATIFIED FLOW	18
COMPUTED EFFECTS OF SHEAR LAYER ON SOUND PROPAGATION	22
Velocity Profile in Shear Layer	22
Ray Paths and Wave Normal Deflection	24
Effective Deflection of Ray Path	27
Sound Pressure Level	29
Intensity	30
CONCLUSIONS AND RECOMMENDATIONS	30
APPENDIX A	33
APPENDIX B	50
APPENDIX C	52
APPENDIX D	54
REFERENCES	57
FIGURES 1 THROUGH 19	59

PROPAGATION OF SOUND THROUGH A SHEARED FLOW

SUMMARY

Sound generated in a moving fluid must propagate through a shear layer in order to be measured by a fixed instrument, whether the microphone is placed in or outside of the flow. Passage through such a shear layer can significantly alter the features of the sound. These alterations must be accounted for if one wishes to characterize the nature of the sound source from such measurements. The present investigation was initiated to provide means of evaluating and correcting for these propagation effects for noise sources typically associated with single and co-flowing subsonic jets and for subcritical flow over airfoils in such jets.

The techniques for describing acoustic propagation fall into two categories; geometric acoustics and wave acoustics. Geometric acoustics has much in common with geometric optics and is most convenient and accurate for high frequency sound. Wave acoustics is generally applicable to sound of all frequencies but is computationally difficult, and valid formulations, much less solutions, are known for only very restricted types of flows.

In the frequency range of interest to the present study (greater than 150 Hz), the geometric acoustics approach was determined to be the most useful and practical method for describing the passage of sound through jets. Calculation methods and a computer program were developed to aid in the interpretation of results. This report describes these results, together with some background information on the general nature of sound propagation through shear layers.

INTRODUCTION

The Ames Anechoic Flow Facility (AAFF) has the potential of providing advance experimental data on a variety of important aeroacoustic phenomena such as subsonic jet noise source characteristics and their suppression, airfoil noise sources (single and cascades), and turbulent scattering of noise. As with any experimental investigation, however, the evaluation and interpretation of the raw measured data is of utmost importance.

Sound generated in a moving fluid such as a jet propagates through a shear layer. Passage through a shear layer can significantly alter the features of the sound. These alterations must be accounted for if one wishes to characterize the nature of the sound source from measurements made by a microphone placed either inside or outside the flow, as will often be the case for studies carried out in the AAFF. With this in mind the present investigation was initiated to provide means of evaluating and correcting for these propagation effects for noise sources typically associated with single and co-flowing subsonic jets and for subcritical flow over airfoils in such jets.

During the investigation the general nature of sound propagation through sheared flows, methods for its description, and experimental data for evaluating those methods were reviewed. The techniques for describing acoustic propagation fall into two categories, namely geometric acoustics and wave acoustics. The former has much in common with geometric optics and is most convenient and accurate for high frequency sound. Wave acoustics is generally applicable to sound of all frequencies but is computationally difficult, and valid formulations, much less solutions, are known for only very restricted types of fluid flows.

In the frequency range of interest in the AAFF (>150 Hz), the geometric acoustics approach was determined to be the most useful and practical method for describing the passage of sound through jets. Calculation methods and a computer program were developed to aid in interpretation of results obtained from the AAFF. This report describes these results, together with some background information on the general nature of sound propagation through shear layers.

NOMENCLATURE

a	isentropic speed of sound in fluid at steady flow
C_1, C_2	constants
$\vec{e}$	unit vector
f	generalized function
F	generalized function
G	generalized function
h	lateral distance from source to longitudinal extension of nozzle lip. In vortex sheet analysis, lateral distance from source to shear layer
H	enthalpy of undisturbed flow
I	acoustic intensity
M_o	Mach number of jet
M_∞	Mach number of ambient fluid outside shear layer
$\vec{n}$	normal to the wave front
p	static pressure of fluid
p'_c	acoustic pressure at location c of figure 2 in absence of shear layer
p'_m	measured acoustic pressure at location of observer
r	radial coordinate
$\vec{r}$	spatial coordinate
R	distance from source to receiver
$\vec{s}$	local distance along ray path
S	entropy of undisturbed flow
t	time
T	static temperature of fluid
$\vec{U}$	velocity of wave front
u,v,w	velocities along x,y,z axes, respectively
$\vec{V}$	undisturbed flow velocity
x,y,z	space-fixed Cartesian coordinate system
X,Y,Z	space-fixed Cartesian coordinate system, rotated 90° about z-axis to xyz coordinate system
β	angle between x axis and projection of $a\vec{n}$ on xy plane
γ	angle between z axis and $a\vec{n}$
η	$-\sigma(Y-Y_o)/(X-X_o)$
θ_c	angle of emission of signal by source in convecting medium
θ_m	measured angle from source to observer, with respect to jet axis
θ_r	angle of reflected wave with respect to jet axis

NOMENCLATURE (Concluded)

θ_s	angle of emission of signal by stationary source, with respect to jet axis
θ_t	angle of transmitted wave (outside shear layer) with respect to jet axis
θ_{zs}	maximum angle of "zone of silence"
ρ	density of fluid at steady flow
σ	spreading rate parameter in shear layer calculations
ϕ	disturbance velocity potential
ϕ_ω	disturbance velocity potential at frequency ω
ω	frequency, sec^{-1}

Subscripts

$( )_o$	mean component
$( )_x$	differentiation with respect to x
$( )'$	fluctuating (acoustic) component

NATURE OF PROBLEM

The general objective of the present study is to develop efficient calculative methods which will facilitate the analysis and interpretation of acoustical data obtained in the AAFF. The general arrangement with which we are concerned is shown in figure 1. A detailed description of the facility and its flow characteristics is given in reference 1.

In more specific terms, the work entails the mathematical interpretation of acoustical signals generated in and propagating through the open jet of the facility, or a portion of it, and measure by microphones in an essentially quiescent medium outside the jet. The investigation is focused on describing the effects of the jet flow on sound propagation. Such effects include not only motion of the medium, but motion of the source of the sound as well.

In delineating the propagation effects, it should be observed that it is not always possible to clearly separate the effects of propagation from those associated with noise generation for real sources of sound. Nor is it always possible to consider the acoustic signal separately from the flow field. In order to obtain useful results, it has been necessary therefore to define carefully the assumptions regarding the sources of sound treated in the present study and the limitations of the resulting methods for describing sound propagation.

In particular, the propagation effects to be considered in the present study include refraction (which is due to gradients in flow velocity and medium properties), convective amplitude and directional shifts, and Doppler effects (due to relative motion of source, medium, and observer). Other effects of the medium, such as source modification by the flowing medium or the generation of additional noise sources due to the effects of noise on the flow are not considered *per se*, but may be included *a priori* as prescribed sources. One further effect is that of sound scattering by turbulence. The state-of-the-art of this effect is such that little quantitative treatment can be reported. Therefore it has not been considered in the present study.

Consider the ray emitted by a stationary source at the angle θ_s in a stationary medium, as shown in sketch (a). If this source were placed in a uniformly moving medium this ray would propagate in the direction θ_c due to convection by the medium, as shown in sketch (b). If this ray propagates through a non-uniformly moving medium, such as a jet shear layer,

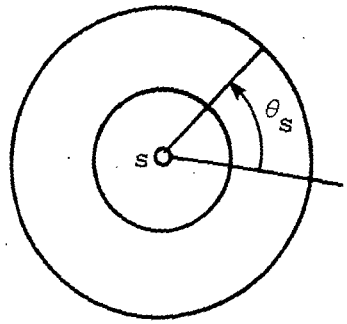

(a) Uniform stationary medium.

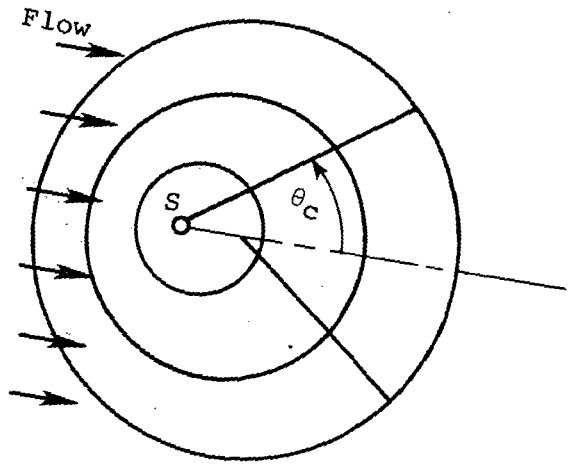

(b) Uniformly moving medium.

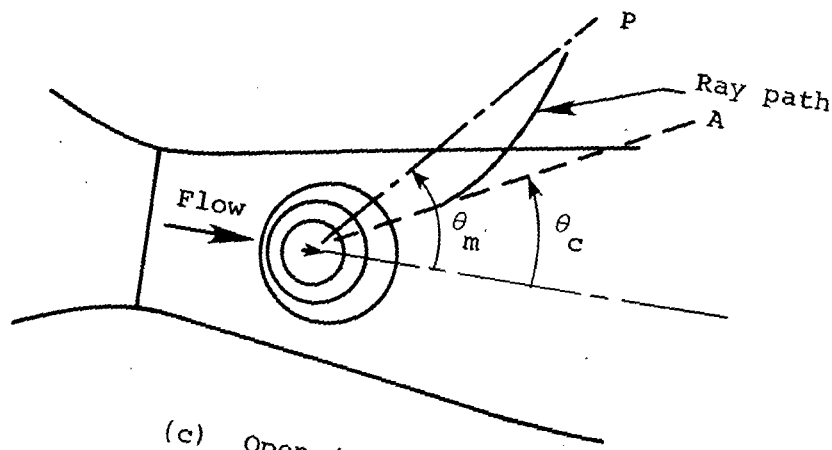

(c) Open jet.

its direction will undergo further changes due to the variations in velocity and speed of sound in that region. This situation is shown in sketch (c).

The several available techniques for describing acoustic propagation were surveyed to determine which had the most attractive features and would be valid for frequencies of interest (i.e. greater than 150 Hz) in the AAFF. These were programmed for computer calculation and some sample calculations were carried out. A satisfactory technique was identified for the geometric acoustics approach. Evalution of the various methods utilizing wave acoustics indicated that the Lilley Wave Operator is probably the best for these purposes. However, the results of a recent comprehensive experimental and analytical study jointly sponsored by the Department of Transportation and NASA (ref. 2) indicate that there is little practical difference between results from this and geometric acoustics for the sound of interest in the AAFF. Amiet (ref. 3) has investigated the short wavelength limit and found geometric acoustics to be acceptable as a correction technique for sound with wavelength less than a jet diameter. Accordingly, the current study has concentrated on providing a satisfactory geometric acoustics calculation technique with provision for examining various sources and source movement effects.

BACKGROUND

A systematic mathematical study of the feasibility of wavelike solutions to the equations of motion has been recently published by Gunzburger and Kleinstein (ref. 4). They have concluded that periodic solutions to the Navier-Stokes equations exist only under very restrictive conditions, many of which are not generally satisfied by shear flows of the type occurring in the AAFF. Hence, short of completely solving the Navier-Stokes equations by some means (e.g. numerically) we cannot expect to totally describe the noise measured in such a facility by theoretical means. It is clear from observation, however, that locally, or for short periods of time, wave-like disturbances do exist in such flow fields under many conditions. In the following, we will briefly discuss some approximate formulations and indicate their theoretical and physical limitations.

Theory

There are several approaches to describing the propagation of sound in homogeneous media. It appears from the present investigation that

wave-like solutions have only been found for the governing equations after linearization for small disturbances. Blokhintsev (ref. 5) showed that the governing equations of inviscid fluid mechanics, linearized for small disturbances, can be expressed in a wave equation form. The frequency, ω, and vorticity (curl $\vec{V}$) for which this development applies is $|\text{curl } \vec{V}|/\omega << 1$. He also discussed the propagation of sound in an irrotational isentropic flow. For such a flow the equation for the disturbance velocity potential, ϕ, is

$$\frac{D^2\phi}{Dt^2} = a^2\nabla^2\phi + \text{grad } H \cdot \text{grad } \phi + \frac{\partial\phi}{\partial t}\vec{V} \cdot \text{grad}(\ell n\ a^2) \qquad (1)$$

where

$a = \left(\frac{\partial p}{\partial \rho}\right)_S$ = isentropic speed of sound in fluid

$\frac{D(\ )}{Dt}$ = substantial derivative $\frac{\partial(\ )}{\partial t} + \vec{V} \cdot \text{grad } (\ )$

H = enthalpy of the undisturbed flow

S = entropy of the undisturbed flow

$\vec{V}$ = undisturbed flow velocity (upon which small acoustic disturbances are superposed)

This equation is recognizable as being related in form to the wave equation. It is a linear, second order differential equation and will support wave-like solutions if the steady flow properties involved in its coefficients are well behaved. In particular, the coefficients in the equation are independent of time; hence, the general solution can be represented in terms of superposed solutions of the form:

$$\phi_\omega = A(\vec{r};\omega)\ \exp(i\omega t) + \text{conjugate} \qquad (2)$$

where

$A(\vec{r};\omega)$ = the complex amplitude and spatial phase function for the ω component

$i = \sqrt{-1}$

$\vec{r}$ = spatial position

t = time

ω = frequency

Schubert (ref. 6) has developed a numerical solution technique for equations like equation (1) applied to a jet flow field. He indicated that his solution method was applicable to either the velocity potential

or Obukhov's potential. However, property gradients were accounted for only approximately. The solution process is tedious, especially when either of the last two terms of equation (1) are retained, and the results obtained by Schubert were little if any better than those obtained from geometric acoustics.

The formulation of equation (1) will permit the extensive examination of sound propagation in flows with fluid property gradients, but the velocity field must be irrotational. The latter restriction excludes shear flows except as they may be approximated using surfaces of concentrated vorticity (vortex sheets) to define their boundaries. Such an approximation would seem to be permissible when the gradients of the steady flow are large compared to those due to the presence of the wave motion, that is, in a long wave length approximation. A discussion of the condition for the validity of this approximation has not been found in the literature, but one should be able to derive those conditions in terms of the wave length of the sound, the thickness of the shear layer, and perhaps the angle of incidence of sound waves on the shear layer (a surface parallel to it). The latter will be made clearer when geometric acoustics is discussed.

Lighthill (ref. 7) subsequently (to Blokhintsev) published his "acoustical analogy" approach, in which the equations of motion were "forced" into the form of a wave equation for a homogeneous, stationary medium. All effects of flow and fluid property inhomogeneities are accounted for by "equivalent source" mechanisms, according to Lighthill's theory. The Lighthill theory, which is exact, models the sound radiation from a flowing fluid as emanating from nonstationary sources in a stationary medium. Thus, all refraction and convection effects of the flow are accounted for by "equivalent" time-dependent sources. This formulation is exact but difficult to apply because the source terms are not exactly known or knowable. The significance of the theories developed since Lighthill is in their attempts to separate more clearly the noise production from the propagation effects of the flow.

The theories of Phillips (ref. 8), Csanady (ref. 9), and Lilley (ref. 10) have attempted to identify the "true source" mechanisms of sound production in terms of commonly recognized fluid and flow properties. They have formulated the problem in terms of various "convected wave" equations. By so doing, they have also contributed to the

isolation of "propagation effects" which may be used to analyze noise radiated through but not generated in a given flow. Doak (ref. 11), Howe (ref. 12), and Yates and Sandri (ref. 13) have constructed theories based on quasi-potential functions which are specifically formulated to separate sound production from sound propagation in inhomogeneous rotational flows.

Each of these formulations is "exact" in the sense that they can be derived directly from the governing equations of fluid motion. Their differences lie in their ability to describe the various acoustics phenomena in terms of known or knowable properties of the fluid medium and its flow field. It is doubtful that any one of these theories will prove to have decisively separated propagation and production effects for all situations.

At present, the most promising wave equation formulation for the current application (i.e., for the study of sound propagation) is that of Lilley. This equation is

$$\frac{D^3q'}{Dt^3} - \frac{D}{Dt}\,\mathrm{div}(a^2\,\mathrm{grad}\,q') + 2\left[\mathrm{div}\,\frac{D}{Dt} - \frac{D}{Dt}\,\mathrm{div}\right](a^2\,\mathrm{grad}\,q') = \text{Source Terms} \qquad (3)$$

where

$q' = \ell n\ p'/p_o$ the natural logarithm of the ratio of the fluctuating (acoustic) pressure to the mean static pressure.

This equation is only valid for parallel mean flows (i.e., flows which are undirectional and have gradients only transverse to that direction). Recent publications of results provide some insight into the capabilities of this method. Balsa (ref. 14) has published results for an arbitrary radial velocity profile with a single point quadrupole moving along the axis of a jet. Tester and Morfey (ref. 15) have considered a ring of quadrupoles at a constant radius and investigated the effects of nonuniform density on sound radiation from jets.

Geometric acoustics is the least restrictive approach in terms of the types of flows which can be examined. It is probably the easiest to understand, also, since it primarily involves kinematical relations among the wave and fluid velocity components to trace so-called "rays", the locus of a point on a wave front as it passes through the fluid. The major restriction of this approach is the assumption that the variation of the properties characterizing the basic initial state over small

distances and short times, compared to a characteristic length (e.g. wave length) and characteristic time (e.g. period) associated with the acoustic field are negligible. Thus, one must expect inaccuracies when the sound frequency is low enough that the acoustic wave length is the order of the shear layer thickness or another characteristic flow dimension.

Acoustic intensity may be calculated by assuming energy conservation within a bundle of rays. This approach ignores the action of viscosity in the wave motion and is thus inaccurate when the rays become focused in a region so as to bring this action into the picture as a significant phenomenon. However, this difficulty is not restricted to geometric acoustics. It is partially an amplitude effect which is not accounted for in most of the other approaches, since they rely on linearization of the acoustic disturbance as well. Geometric acoustics is also inaccurate if the acoustic disturbance generates further acoustic energy by interaction with the flow (e.g., triggering flow instability). Since this is in effect creating new sound sources, this shortcoming is also present in other approximate methods.

While some theoretical limitations can be identified, a comprehensive evaluation of existing theoretical methods is difficult at best due to the lack of well defined experimental measurements. This situation is discussed in the following section.

Experiment

There have been numerous experimental investigations of the directional distribution (directivity) of sound in the presence of jet flows. These measurements have been used to evaluate the several aeroacoustic noise theory formulations. However, only in the investigations at the University of Toronto [Atvars, et al. (ref. 16) and Grande (ref. 17)] was the source adequately characterized so as to make the measurements conclusively useful for evaluation of flow-acoustic propagation effects. In other investigations the sound source was estimated based on the particular aerodynamic noise theory under study. The actual nature of the source in the presence of the medium was generally only estimated. While there is no strong evidence that a flowing medium does anything unexpected to a source, neither is there conclusive evidence that it doesn't. In light of the recent disclosures by Dowling (ref. 18) regarding the

physical concept of the "ideal" source in the presence of a moving medium, caution, at least, is suggested.

Although ray tracing techniques are supposedly limited to short wavelengths, they appear to give reasonably supportable results for most frequencies of interest in wind tunnel testing except for passage through the shear layers at large angles with respect to the normal to the shear layer (e.g., shallow angles with respect to the jet axis). Further, Amiet (ref. 3) has investigated the short wavelength limit of geometrical acoustics and found it to be acceptable for wavelengths less than a jet diameter.

Balsa (ref. 14) and Tester and Morfey (ref. 15) evaluated the results of their calculations of flow-acoustic interaction based on the Lilley formulation of the wave operator. Each of these studies indicated difficulties in comparison with experimental results (theirs and others) at both low and high frequencies and at small angles to the jet axis. Also, a recent analytical and experimental study (ref. 2) has concluded that predictions from the Lilley equation for propagation angles outside the so-called "zone of silence" can be closely approximated with results from calculations using geometric acoustics.

Since calculations by geometric acoustics are straightforward (if somewhat tedious algebraically) and the zone of silence is not of primary significance in the Ames Anechoic Flow Facility, the efforts have concentrated on development of a generally applicable geometric acoustics ray tracing computer program. This approach is applicable to any flow field property distribution within the short wavelength restriction, as well as to any of the "ideal" source types. The Lilley equation, with its restricted applicability may be employed as a check on the low frequency limitations of the geometric acoustics approach.

THEORETICAL BASIS OF GEOMETRIC ACOUSTICS

Kinematics of Wave Propagation in a Three-Dimensional, Inhomogeneous, Moving Medium

The fundamental approach is to describe the motion of a wave front locally in terms of the fluid properties and motion, but require that the motion conform to Fermat's stationary transit time principle. A general derivation based on geometric acoustics may be found in Ugincius

(ref. 19). The present derivation uses only wave front kinematics and Fermat's Principle to derive the governing equations.

The fundamental mechanics of wave propagation require that a wave front move relative to the medium with the local speed of sound $a(\vec{r})$. The wave front will additionally be convected by the local velocity $\vec{V}(\vec{r})$ of the medium, yielding a total velocity of the wave front, $\vec{U}(\vec{r})$. This can be expressed as

$$\vec{U}(\vec{r}) = \vec{V}(\vec{r}) + a(\vec{r})\ \vec{n}(\vec{r}) \tag{4}$$

where

$$\vec{U}(\vec{r}) = \frac{d\vec{r}_s}{dt} = \frac{ds}{dt}\vec{e}_s$$

where

$\vec{r}_s(t)$ = the location of an element of the wave front at time t (as shown on the next page)

s = the distance along the ray

$\vec{e}_s$ = the unit vector tangential to the ray path at $\vec{r}_s(t)$

The velocity components of the element of the wave front in the x, y, and z directions are given, respectively, by the following equations.

$$\frac{dx}{dt} = u + a \sin\gamma \cos\beta \tag{5}$$

$$\frac{dy}{dt} = v + a \sin\gamma \sin\beta \tag{6}$$

$$\frac{dz}{dt} = w + a \cos\gamma \tag{7}$$

where

$$\sin\gamma \cos\beta = \vec{n} \cdot \vec{e}_x$$
$$\sin\gamma \sin\beta = \vec{n} \cdot \vec{e}_y$$
$$\cos\gamma = \vec{n} \cdot \vec{e}_z$$

If we take one of the variables, say x, as the independent variable, the above equations may be combined to eliminate the time t and the angles γ and β, which indicate the local wave normal direction.

$$z_x = \frac{dz}{dx} = \frac{dz/dt}{dx/dt} = \frac{w + a\cos\gamma}{u + a\sin\gamma\cos\beta} \tag{8}$$

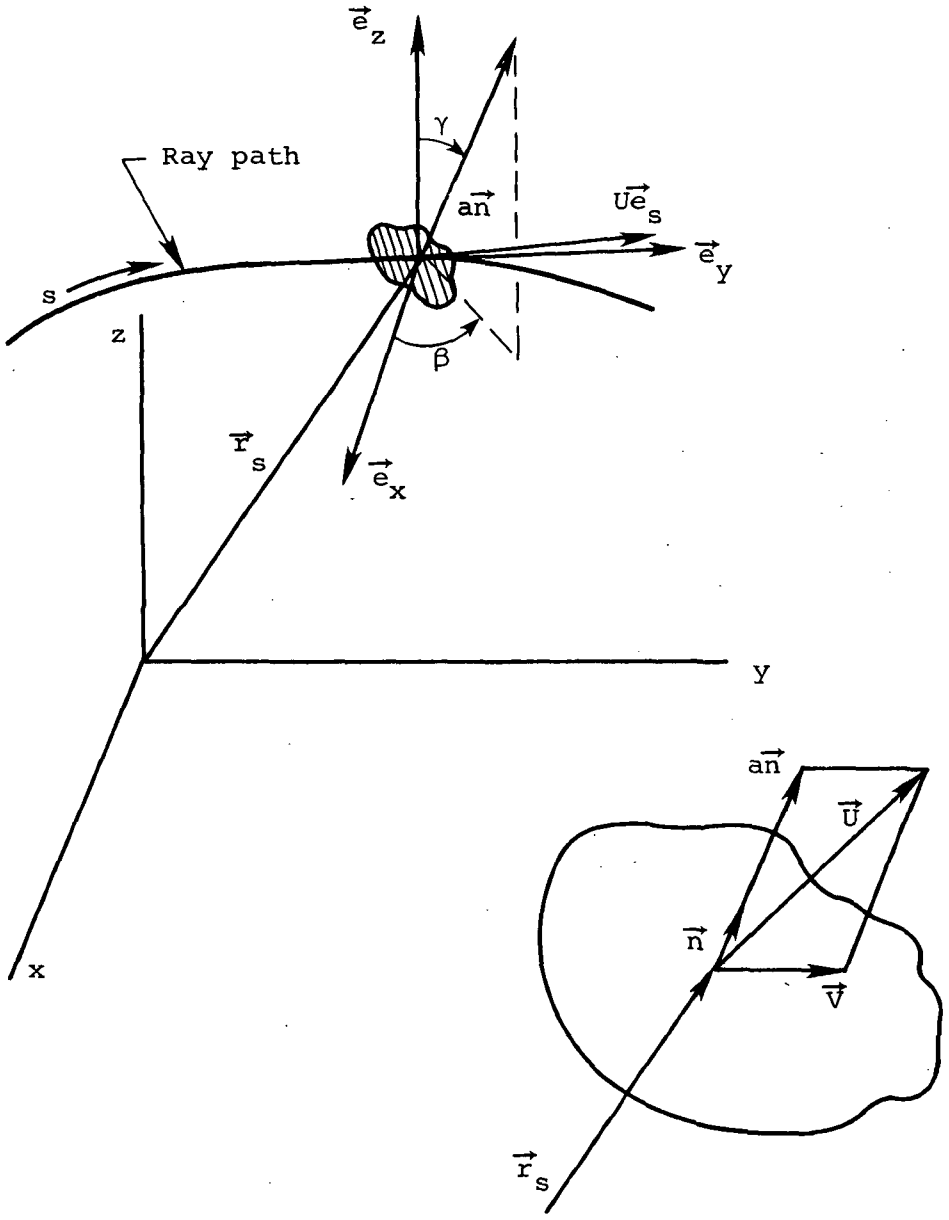
$\vec{e}_z$
γ
Ray path
$\vec{an}$
$U\vec{e}_s$
$\vec{e}_y$
s
z
β
$\vec{r}_s$
$\vec{e}_x$
y
x
$\vec{an}$
$\vec{U}$
$\vec{n}$
$\vec{V}$
$\vec{r}_s$

$$y_x = \frac{dy}{dx} = \frac{dy/dt}{dx/dt} = \frac{v + a \sin \gamma \sin \beta}{u + a \sin \gamma \cos \beta} \tag{9}$$

The following useful relations can be derived from equation (8) and (9).

$$a \cos \beta = \frac{-(z_x u - w) \pm a \cos \beta}{z_x \sin \gamma} \tag{10}$$

and

$$a \cos \beta = \frac{-y_x(y_x u - v) \pm \sqrt{a^2 \sin^2 \gamma (1 + y_x^2) - (y_x u - v)^2}}{(1 + y_x^2) \sin \gamma} \tag{11}$$

Letting

$$V = y_x u - v \tag{12}$$

$$W = z_x u - w \tag{13}$$

It can be shown that

$$a \cos \beta = \left\{ \left[W(1 + y_x^2) - y_x z_x V \right] \left[\pm z_x \sqrt{\frac{(1 + y_x^2 + z_x^2)\,[a^2(1 + y_x^2) - V^2] - [W(1 + y_x^2) - y_x z_x V^2]}{(1 + y_x^2)}} \right] \right\} \Big/ (1 + y_x^2 + z_x^2) \tag{14}$$

The appropriate signs may usually be determined by requiring that the direction of propagation remain continuous in a continuous medium.

The Variational Problem and Its Solution

The kinematics of propagation can be determined from the above equations provided any two of γ, β, y_x, or z_x are known along the path of propagation and the properties of the medium (including its flow field) are specified. It is likely that the wave normal or path direction will only be known at an end point. However, the path actually traveled by a "ray" is usually to be determined. A relation for making this determination is provided by a very simply stated principle due to Fermat. Fermat's Principle states that the time required for a ray to travel

between two points will be an extremum. This principle may be formulated as a problem in variational calculus.

The time required for a wave to travel from a position, $s_o(x_o,y_o,z_o)$, on a ray path to another position $s_1(x_1,y_1,z_1)$ is specified by

$$t = \int_{s_o}^{s} \frac{ds}{(ds/dt)}$$

$$= \int \frac{(ds/dx)\,dx}{(ds/dx)(dx/dt)}\Bigg|_{s_o(x_o,y_o,z_o)}^{s_1(x_1,y_1,z_1)}$$

$$= \int \frac{dx}{(dx/dt)}\Bigg|_{s_o(x_o,y_o,z_o)}^{s_1(x_1,y_1,z_1)}$$

$$t = \int \frac{dx}{u + a \sin\gamma \cos\beta}\Bigg|_{s_o(x_o,y_o,z_o)}^{s_1(x_1,y_1,z_1)} \tag{15}$$

By combining equations (6), (10) or (11), (12), (13), and (14), it can be observed that equation (15) may be written

$$t = \int_{s=s_o(x_o,y_o,z_o)}^{s=s_1(x_1,y_1,z_1)} f(x,y,z,y_x,z_x)\,dx \tag{16}$$

with x the independent variable. It can also be shown by the principles of calculus of variations that t is an extremum in equation (16) if f satisfies the simultaneous Euler-Lagrange equations given below. (The extremum is in fact a minimum.)

$$\frac{\partial f}{\partial y} - \frac{d}{dx}\frac{\partial f}{\partial y_x} = 0 \tag{17}$$

$$\frac{\partial f}{\partial z} - \frac{d}{dx}\frac{\partial f}{\partial z_x} = 0 \tag{18}$$

The solutions of these simultaneous equations cannot be given in general, but can be obtained if f has certain properties.

It will be observed that the only explicit dependence of f on x, y, and z arises from the properties of the medium, $\vec{V}(x,y,z)$ and $a(x,y,z)$.

If these properties are constant, equations (17) and (18) reduce to

$$\frac{\partial f}{\partial y_x} = C_1 \qquad \frac{\partial f}{\partial z_x} = C_2$$

which will yield the familiar relations for propagation in a homogenous medium.

Equations (17) and (18) are valid generally, however, and may be used to determine the path of a ray in an inhomogeneous medium. We will now discuss briefly the general features of these equations.

In carrying out the indicated operations of equations (17) and (18), one will arrive at two equations (Euler-Lagrange) of the forms

$$F(x,y,z,y_x,z_x,y_{xx},z_{xx}) = 0 \tag{19}$$

$$G(x,y,z,y_x,z_x,y_{xx},z_{xx}) = 0 \tag{20}$$

Equations (19) and (20) represent coupled, second-order differential equations for the ray path. Their general solution will have four arbitrary constants, which one may reason will permit specification of a corresponding number of the following:

1. Initial point of ray, $s_o(x_o,y_o,z_o)$
2. Final point of the ray, $s_1(x_1,y_1,z_1)$
3. $(y_x)_o$ or β_o
4. $(z_x)_o$ or γ_o
5. $(y_x)_1$ or β_1
6. $(z_x)_1$ or γ_1

Rarely is it expected to be able to determine the general solutions to (19) and (20) in an analytical form, but they may be employed to provide an estimate of y_x and z_x or β and γ along the path by performing a numerical integration of each. Then, if one is given an initial point (x_o,y_o,z_o) and wave normal direction (β_o, γ_o, or y_x, z_x) the ray path may

be constructed in a stepwise manner by specifying $dx = \Delta x$, calculating Δy and Δz from the initial information and Δx. New values of y_x and z_x (β and γ) may then be determined by integrating equations (19) and (20) and used to compute the next increment along the ray path by repeating the previous process.

SOUND PROPAGATION IN A STRATIFIED FLOW

As a first approximation in the analysis of shear layer effects on acoustic propagation the actual shear layer can be replaced by one of zero thickness - a vortex sheet. This simplified flow model provides quick, inexpensive results. Historically, the first attempts to correct wind tunnel acoustical measurements for the effects of a shear layer were performed by Amiet (ref. 20) and Jacques (ref. 21) utilizing this approach. Physically, a vortex sheet is not a realistic representation of a shear layer in a typical wind tunnel jet flow. Under certain conditions however, comparisons between theoretical and experimental results are in close agreement. Thus, under these conditions, which will be discussed shortly, the vortex sheet assumption is an attractive alternative.

This method has several other advantages in addition to quick and reasonable results. First of all, the corrections for shear layer effects are obtained as straightforward multiplicative factors of the measured amplitude and position, independent of source type or frequency. In addition, when re-analyzing previous data for which shear layer characteristics were not measured, an assumption of this type is the only one possible. However, there are also several equally distinct disadvantages to this model that are a direct result of the assumption of zero shear layer thickness. Among these disadvantages are the prediction of a portion of the incident acoustic energy being reflected from the shear layer interface and the prediction of a so-called "zone of silence". Before discussing these effects in detail a brief physical description of the vortex sheet model shall first be presented.

The vortex sheet model of the flow is shown in figure 2. An acoustic source at point s imbedded in a fluid flowing uniformly at Mach number M_o emits waves at an angle θ_s with respect to the flow axis. (For simplicity, the discussion will be limited to consideration of plane

waves but the model does not strictly require this assumption.) Due to convective effects of the flow the waves propagate along a path at an angle θ_c to the flow axis. No further assumptions regarding the source are required. The boundary between the moving fluid and the ambient outer fluid is idealized by a velocity discontinuity - the vortex sheet. The interaction between an incident wave and a plane interface has been discussed previously by, among others, Ribner (ref. 22). The major features only will be summarized here. When the incident wave reaches the interface a portion of the energy is transmitted into the ambient fluid at an angle θ_t and a portion is reflected back into the moving fluid at an angle θ_r. The transmitted wave eventually reaches an observer located at position 0. Hence, the wave reaching the observer is different, both in magnitude and in direction, than the emitted wave. The objective then is to reconstruct the emitted signal from the received signal.

In the absence of the shear layer the signal would continue to propagate at the angle θ_c, eventually reaching the point c, the same distance r from the source as the point 0. Actually, the corrections can be determined for any point along the convected path, as shown by Amiet (ref. 20). The properties of refraction at an interface can then be used to determine the relation between θ_m, the measured directivity angle, and θ_c, the convected directivity angle.

The determination of the corrected amplitude at the point c is slightly more complicated. To the effects of refraction by the shear layer on the amplitude must be added the effects of geometric spreading. This includes spreading in both the xy plane and the xz plane. These effects are determined by considering the spreading of a ray bundle as it crosses the interface and assuming that the shear layer neither absorbs acoustical energy from the ray tube nor generates additional acoustical energy through interaction with the flow. However, Koutsoynnis (ref. 23) casts severe doubt on this assumption. It is quite apparent that additional work is required, including careful experiments on the effects of propagating acoustic waves on shear layer stability.

The vortex sheet approach previously has been investigated by Amiet (ref. 20) for a plane shear layer and by Jacques (ref. 21) for a cylindrical shear layer. Some features of sound wave interaction with a plane shear layer will be investigated here. Comparisons of the various

correction terms due to the plane and cylindrical shear layers have been examined by Amiet (ref. 3).

At the interface the boundary conditions to be satisfied are (1) continuity of pressure across the interface and (2) the velocity is tangential to the surface of the interface. With these assumptions the relation between the measured directivity angle and the convected directivity angle is found to be

$$\sin \theta_m = \frac{\xi \cot \theta_t}{1 + \cot^2\theta_t} + \frac{[(2\xi\cot\theta_t)^2 - 4(\xi^2 - 1)(1 + \cot^2\theta_t)]^{1/2}}{2(1 + \cot^2\theta_t)} \tag{21}$$

where $\xi = \frac{h}{R} (\cot\theta_c - \cot\theta_t)$ (22)

$$\theta_t = \frac{1}{(1 - M_o^2)} \quad \frac{\cos \theta_c}{[1 - M_o^2\sin^2\theta_c]^{1/2}} - M_o \tag{23}$$

Notice that the relative locations of source and observer with respect to the shear layer enter into the relation. It can be shown that

$$\lim_{h/R\to o} \quad \theta_m = \theta_t \tag{24}$$

Including the effects of both refraction and geometric spreading the amplitude correction is given by

$$\frac{p'_c}{p'_m} = \frac{\csc \theta_t}{\zeta^2} [\frac{h}{R} \sin \theta_t + (\sin \theta_m - \frac{h}{R})\zeta]^{1/2} [\frac{h}{R} \sin^3\theta_t + (\sin \theta_m - \frac{h}{R})\zeta^3]^{1/2}$$

$$\frac{1}{2\sin\theta_t} [M_o^2(1 - M_o\cos\theta_t)^2 + (1 - M_o^2\cos\theta_t)]^{1/2} [\zeta + \sin\theta_t(1 - M_o\cos\theta_t)^2] \tag{25}$$

where

$$\zeta = [(1 - M_o\cos\theta_t)^2 - \cos^2\theta_t]^{1/2} \tag{26}$$

This relation can also be evaluated for the effects of small h/R. If this is done,

$$\lim_{h/R \to 0} \frac{p'_o}{p'_m} = \frac{1}{2\sin\theta_t} [M_o^2(1 - M_o\cos\theta_t)^2 + (1 - M_o^2\cos^2\theta_t)]^{1/2}$$

$$[\zeta + \sin\theta_t(1 - M_o\cos\theta_t)^2] \tag{27}$$

There are two important angles that appear in the vortex sheet analysis. The first angle is the value of θ_t corresponding to $\theta_c = 0$, which can be shown to be

$$\theta_{zs} = \cos^{-1}\frac{1}{1 + M_o} \tag{28}$$

This relation is shown in figure 3. The physical significance of this angle is that no sound waves propagate in the outer field at angles less than θ_{zs}. The second angle is that value of θ_c for which sound waves that are emitted at angles greater than this are totally reflected. This angle corresponds to $\theta_t = \pi$ which is

$$\theta_{tr} = \cos^{-1}(-\frac{1}{1 + M_o}) \tag{29}$$

Hence, sound waves emitted at angles $\theta_c > \theta_{tr}$ are totally reflected and cannot be received by an observer outside the shear layer. Values of θ_{tr} are shown in figure 4.

These concepts are shown in figure 5 for three different Mach numbers. As can be seen, at a flow Mach number of 0.9 only the sound emitted over the forward quadrant propagates through the shear layer according to the vortex sheet model. The rest is reflected back into the flow.

COMPUTED EFFECTS OF SHEAR LAYER ON SOUND PROPAGATION

A computer program was generated to carry out the indicated geometric acoustics procedures for three-dimensional wave propagation from a fixed

source in a two-dimensional flow and fluid property field. The program is described in Appendix A.

It should be noted that the coordinate system (X,Y,Z) in which the user communicates with the program is rotated 90° about the z-axis compared to that in the previous derivation (x,y,z). See the sketch below.

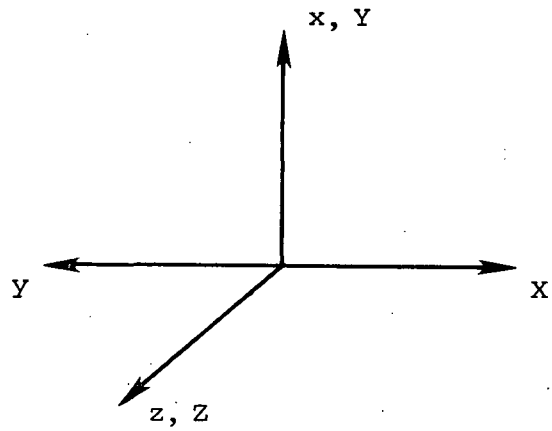

This has in effect substituted Y for X as the independent variable and made angular computation using the standard computer system library subroutines more convenient when the major flow velocity is in the X direction.

Calculations using the program were carried out for a two-dimensional isothermal shear layer. Sample results are presented for a range of Mach numbers from 0.2 to 0.9 and wave normal angles (at the source) from 30° to 120° with respect to the flow direction and in the plane of the flow. Various features of the sound propagation were determined and are presented in the following discussion.

Velocity Profile in Shear Layer

The two-dimensional velocity profile used in all calculations was the hyperbolic tangent profile:

$$u = \frac{u_o}{2} (1 + \tanh \eta) \tag{30}$$

$$v = \frac{u_o}{\sigma} (\eta \tanh \eta + \ell n \frac{\operatorname{sech} \eta}{2}) \tag{31}$$

where $\eta = -\sigma\ (Y - Y_o)\ (X - Y_o)$

u = X-component of velocity, the main flow direction

v = Y-component of velocity

u_o = reference velocity

σ = spreading rate parameter

The general features of this velocity profile are shown in figure 6. This is a self similar, nonparallel flow with a small but finite transverse velocity. The relation for the transverse component of velocity, v, given by equation (31) has been computed from equation (30) and the continuity equation for a two-dimensional, incompressible flow. The condition that $v \to 0$ far from the shear layer was also used.

Practical limits on η were invoked for calculation purposes and the flow was considered to be uniform and parallel outside of $|\eta| = 6$ in the present calculations.

The spread parameter, σ, sets the spatial scale of the flow. In particular, it and the velocity, u_o, determine the shearing rate for the flow. A value of $\sigma = 15.2$ was used in the sound propagation calculation presented in this report. This value was chosen to match the maximum rate of shear of another velocity profile (the error function) used in a referenced report (ref. 2). Propagation data and calculations from this report were used for comparison with the present calculations.

The velocity is not used directly in the ray path calculations. It is the ratios of the velocity components to the local speed of sound, a, which are directly involved. These are denoted by $M_{xx}=u/a$ and $M_{yy}=v/a$.

The present calculations were carried out for an isothermal flow in which the speed of sound was a constant, a_o, throughout. The ratio u_o/a_o is denoted by M_o in the text and figures. Appendix B contains expressions for generalizing the calculation directly to a fluid obeying the Crocco relation between velocity and temperature. These were not examined in the present calculations. However, the computations themselves are well within the scope of the included theory. In fact the main program can handle three-dimensional wave propagation in any physically realistic, two-dimensional density and speed of sound variation one would wish to input in the subroutine provided for the flow and fluid properties. As a final note it should be mentioned that the ray path is not dependent directly on fluid density.

Ray Paths and Wave Normal Deflection

The typical features of the ray paths predicted by the present method are examined in this section. In order to facilitate interpretation and comparison with other data the results presented will be for components of waves in the plane of the flow containing the maximum velocity gradient. No two-dimensional wave approximations have been employed in the calculations, however. The program has the capability of treating three-dimensional wave surfaces in a two-dimensional medium, as previously stated.

When considering the directional pattern of sound radiating from a source in a moving medium some authors prefer to use the convected emission angle, θ_c, or the ray path angle as the independent variable. In the present investigation, the wave normal emission angle, θ_s, that is the angle relative to the x-axis, has been used. It is believed this will facilitate later investigations involving source motion and non-uniform source emission. If the flow is uniform the relation between these angles in the plane of the flow is particularly simple. As an aid in comparing the present results to those of other investigations, this conversion is illustrated in figure 7 for several subsonic Mach numbers.

The appearance of the ray paths for various wave normal angles between 30° and 120° are shown in figure 8. The flow field is the isothermal, hyperbolic tangent flow described in the previous section with $M_o = 0.2$. The lines in figure 8 marked $\eta = \pm 6$ designate the shear layer boundaries. The paths are in agreement with those of Plumblee et al. (ref. 2) and are also very close to those predicted by vortex sheet methods, e.g., the method of Amiet (ref. 20) presented elsewhere in the report.

Plumblee et al. (ref. 2) have indicated that ray paths may be very closely approximated by placing a vortex sheet at the center of the shear layer ("nozzle lip line"). The present results confirm this indication for sources situated in a uniform flow bounded by a thin shear layer. The implication that the thickness of the shear layer or the particulars of the velocity distribution have little effect on the ray path appears to be confirmed at this Mach number by the present calculations. The effects of thickness at higher Mach numbers are shown to be significant, however.

In figure 9 ray paths are shown for $\theta_s = 30°$ for three sources located variously in shear layers having $M_o = 0.2$, 0.5, and 0.9. Sources 1 and 2 are located in the uniform flow region but the corresponding rays from source 2 travel through a much thicker shear layer than do those from source 1. Ray paths for $\theta_s = 30°$, 60°, 90°, 105°, and 120° through the thicker shear layer from source 2 are shown in figures 10-12 for $M_o = 0.2$, 0.5, and 0.9, respectively. The total deflection of the corresponding rays across the entire shear layer was calculated to be within 0.5 degree and generally within 0.2 degree for the two source locations. Seldom would input flow field information be accurate enough to distinguish between these angles.

Figure 13 shows the calculated wave normal deflection angles, $\theta_t - \theta_s$, versus initial wave normal angle, θ_s, at source 1 for $M_o = 0.2$, 0.5, and 0.9. Also shown are the deflection angles calculated from simple vortex sheet methods described elsewhere in this report and the predictions of Plumblee et al. (ref. 2). The latter are for a parallel flow with $M_o = 0.2$ only. All results are in very close agreement for the $M_o = 0.2$ case (less than 1/2 degree spread). The agreement between the present predictions and the vortex sheet is also excellent at $M_o = 0.5$ and for $\theta_s = 30°$ and 60°. Some significant differences show up at 90°, 105°, and 120° for the higher Mach numbers. The maximum difference is about 2 1/2° out of 7° for $\theta_s = 105°$ and $M_o = 0.9$. The deviation at 90° is expected due to the non-parallel flow in the present calculation. However, it is not clear that this can account for the greater deviation for an angle above 90°. Such differences could be the result of a lack of convergence of the numerical solution to the ray equations. The results of the convergence tests performed would not seem to support this, however, and the difference is unexplained as of now.

Thus, the wave normal deflection can be obtained with good accuracy at low Mach numbers or low angles from a simple vortex sheet representation of the shear layer. The representation at high subsonic Mach numbers and angles greater than 90° may be tolerable if the flow is parallel. The extension of this simplified procedure to a shear layer in which the speed of sound as well as the velocity varies requires prior examination to determine if it is valid. Such examination has not been performed here but could be carried out with the present computer program.

If the source is located in a nonuniform region such as the shear layer, the simplified procedure is not available because of the indefi-

nite location of the vortex sheet, regardless of any other shortcomings which may be present. Source 3 of figure 9 is located on the maximum shear line of the velocity profile. The ray paths shown are for the same source angle ($\theta_s = 30°$) and Mach numbers (0.2, 0.5, 0.9) as for source 1 and 2. However, the local Mach number at source 3 is one half of M_o. It is seen that the transmitted ray inclinations are not as great as their counterparts for sources 1 and 2 and examination shows that neither do they approximate those obtained from a vortex sheet of strength 1/2 M_o. Hence, the vortex sheet approximation does not appear to be useful for a source located in a region of shear.

There is another important point of contrast between the present calculation and the vortex sheet. It arises directly from the inadequacy of the vortex sheet in representing the flow geometry. The vortex sheet can intercept only rays which are inclined toward it. The ray which is parallel to the sheet is bent into the surrounding medium at a finite angle defined by equation (28).

Thus, in the vortex sheet approach, no sound can cross the sheet and have a wave normal angle less than $\cos^{-1} \frac{1}{1+M_o}$. The region of wave normal angles θ_{zs} has been, somewhat misleadingly, termed a "zone of silence". This term should not be taken to mean that there is a region in which no sound from the moving side of the vortex sheet can reach it, because that is dependent on the location of the source.

Real shear layers grow however. Specifically, they grow toward the source and can intercept any ray which diverges from the "lip line" less rapidly than does the nearest "boundary" of the shear layer. Hence, all such rays can be turned toward the other side of the shear layer and may emerge from it if the shear layer extends far enough downstream.

No illustrative calculations were made in the present study to specifically examine the "zone of silence" by the present method. However, it would be instructive to do so. In particular it would be interesting to find out whether the deflection relations for the vortex sheet are accurate in this region at low Mach numbers as they appear to be outside it. In the process one could find out where the accuracy of the relations breaks down, if it does. A similar study on the upstream reflection boundary might also prove of interest, although limitations of the vortex sheet model which are soon to be made apparent may prejudice such an investigation.

Effective Deflection of Ray Path

It is often of interest to know the angle of emission of sound reaching a microphone from a source at a known position. This would be extremely important, for example, if the source is directional.

The relative positions of the source and microphone when they are both located in the plane of flow can be specified by the radial distance separating them, R, and the measured angle, θ_m, from the flow direction (i.e. the X-axis) to the straight line connecting the source and microphone. This situation has been examined for sources 1 and 2 (shown in figure 9). The effective deflection angles, $\theta_m - \theta_s$, for sources 1 and 2 are shown in figures 14 and 15, respectively, and compared with results obtained in each case from the vortex sheet model. The parameter h/R is used in the vortex sheet model, but the comparisons primarily reflect "thin" vs. "thick" shear layer effects. For the thin shear layer as in the case of source 1, the vortex sheet calculations agree very well with those of the present method, although some deviation near the 90° emission angle is noted. As previously indicated, this deviation is probably due to the nonparallel flow included in the present calculations.

For the thick shear layer, as in the case of source 2, there are large differences between the present method and the vortex sheet calculations presented. The latter calculations assumed the vortex sheet location to be on the $\eta = 0$ line. It is this assumption which causes the discrepancy. Since both the incoming angle, θ_c, and the outgoing angle, θ_t, are identical or in very close agreement for the two methods, only a displacement of the ray within the shear layer could cause a variance between the two. The following will serve to illustrate this fact.

It is clear that the vortex sheet can be located somewhere within the shear layer it represents and yield good results for the ray path since it reproduces the exit angle θ_t accurately. The proper position of the vortex sheet can be identified a posteriori by extrapolating the straight line positions of the ray path calculated by the geometric acoustics method to their intersection (see sketch).

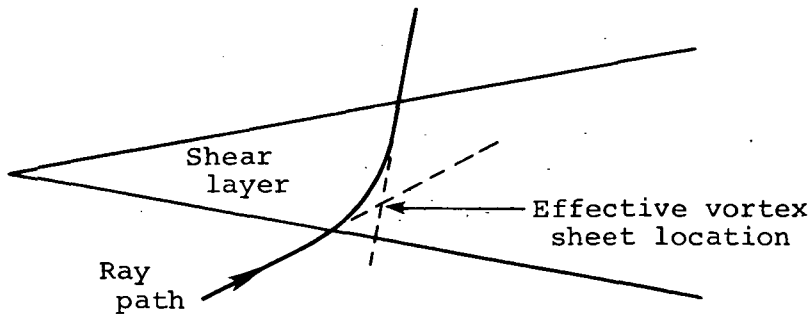

If the shear layer is thin, as for source 1, the error in position cannot be great, therefore the agreement is quite good with an arbitrary positioning of the sheet. The thicker shear layer presents a larger field for error and the error realized is very noticeable in some cases, as shown in figure 15. This represents a clear limitation of the vortex sheet model. This limitation plus the limitations in predicting sound pressure level make it seem not to be worthwhile to determine a pattern for locating the effective vortex sheet position.

Sound Pressure Level

Sample calculations of sound pressure level and intensity relative to appropriate reference values are presented in figures 16-19. In order to continue comparisons with the vortex sheet model developed by Amiet (ref. 20), the sound pressure level is referenced to that which would be measured at an equal radius from the source if the shear layer were absent. This reference condition is called the "Ideal Wind Tunnel" condition by Plumblee et al. (ref. 2). The physical situation is as shown in the sketches in figures 15 and 16. The SPL (Sound Pressure Level) for the thin shear layer associated with source 1 is shown in figure 16 for Mach numbers of 0.2, 0.5, 0.9 and for the range of emission angles, θ_s, from 30° to 120°. The same calculations for the thick shear layer associated with source 2 are presented in figure 17. In both cases it is seen that the shear layer causes a sound pressure increase for those rays emitted in the flow direction ($\theta_s < 90°$) and a decrease for those emitted in a rearward direction with respect to the flow. The change is seen to increase with increased Mach numbers, as would be expected. In comparing the two figures it is noted that the thin shear layer has the greater effect. This is particularly so for small angles

with respect to the flow direction. These results have been compared with the vortex sheet model previously described and those calculations are indicated on the figure. While the general trends are in agreement except for small angles with respect to the flow direction (i.e., approaching the "zone of silence"), the magnitude of the change in SPL is much greater than predicted by the vortex sheet model.

Even though the ray path results using the present and the vortex sheet methods are reasonably comparable for the thin shear layer, the sound pressure results are significantly different. It is believed that the extreme reduction in predicted sound pressure for the vortex sheet model is due to the reflected energy inherent in that method. The reflected wave arises solely from the discontinuity in properties of the medium (including velocity). If the medium properties are continuous, as they physically are, there is no reflected wave. In fact, Amiet (ref. 3) has introduced a "correction" to the vortex sheet model for shear layer thickness which essentially eliminates the effects of the reflected wave. The only "reflection" which appears in the continuous property case is due to sufficient refraction of the rays which enter the bounding region (e.g. shear layer) such that they bend and re-emerge from the same side. This can occur for upstream radiation at a large angle or for large gradients in the speed of sound in the direction of propagation.

Intensity

The sound intensity is affected by propagation through a shear layer in much the same manner as the sound pressure level. The direct relation between sound intensity and pressure is shown in Appendix C of this report. In each case, the effect is minimum for emission at 90° to the flow. It is often of interest to compare the intensity at a point outside the shear flow with that which would be measured at an equal distance from a non-directional source of equal strength but emitted perpendicular to the flow. Such results calculated by the present method are presented in figures 18 and 19 along with a sketch of the physical arrangement of the intensity measurements being compared. Again, these present calculations are for the thin and thick shear layers associated with sources 1 and 2, respectively. As expected the results are much the same in character as those for the sound pressure level shown previously.

CONCLUSIONS AND RECOMMENDATIONS

The features of sound propagation of most importance in interpreting measurements in the Ames Anechoic Flow Facility have been examined. A distinction was made here between sound propagation effects and those of other acoustic and flow interactions. Propagation effects were restricted to those involving convection and refraction of the acoustic signal and relative motion of the source and observer.

Methods for evaluating the propagation effects were discussed and the more promising methods evaluated. The two most accurate methods were those based on geometric acoustics. The vortex sheet method was examined and found to have serious shortcomings, especially at Mach numbers greater than 0.2.

While the Lilley Equation is strictly applicable only to parallel flows, it is valid for all frequencies of interest. Numerical calculations of sound propagation based on the Lilley Equation have been developed by many investigators, e.g., Plumblee et al. (ref. 2), Mani (ref. 24), and Tester and Burrin (ref. 25). Such solutions are frequency and source type (i.e monopole, dipole, quadrupole, etc.) dependent. The geometric acoustics method is generally applicable to all flow fields but is restricted to wavelengths short compared to significant length scales of the medium. A combination of these two methods is recommended to evaluate the range of data obtained in the AAFF.

Because of its generality the major emphasis of the investigation was placed on the geometric acoustics approach which intrinsically is independent of source type and frequency. The equations of geometric acoustics were formulated from the kinematics of "ray" trajectories and Fermat's Principle of stationary transit time.

A computer program was developed in the present study for numerically solving the Euler-Lagrange Equations resulting from Fermat's Principle applied to three-dimensional waves in a two-dimensional, inhomogeneous medium. Sample calculations were carried out for a source in a uniformly moving medium for a range of Mach numbers from 0.2 to 0.9 and sound emission at angles of 30° to 120° with the flow direction. The program traces a ray from a source to a constant radial or side line distance from an arbitrary, specified point. Ray paths, sound pressure and intensity were computed for "bundles" of these rays traversing a

shear layer into a quiescent, uniform medium. Isothermal flow was used for these calculations but the program is not limited to constant sound speed or density. The results of these computations were used to discuss the difficulties in using vortex sheet methods when: (1) the source is located in the shear layer, (2) the shear layer is not small with respect to the acoustic wavelength (i.e. a thick shear layer), and (3) the changes in sound pressure level are being determined.

It is also shown (see Appendix D) how to apply the computational methods to a moving source, as one may have if, for example, it is convected with the flow.

In setting up and analyzing experimental studies it is recommended that the geometric acoustics program be used to locate microphones by predicting the sound propagation features from the sources under investigation and any other major noise sources. A check of the lowest frequencies of interest might also be made using one of the Lilley Equation techniques for comparison. Corrections can be made or seen to be necessary at these low frequencies. Generally, if the wavelengths of interest are less than three times the thickness of the shear layer to be traversed the corrections are negligible (ref. 3).

It is recommended that further work be carried out to expand the capabilities of the computer program developed in this investigation and to use it in combination with an experimental program in the AAFF for clearly defining the limitations of geometric acoustics and evaluating corrections necessary. The only significant modification of the computer program which is seen to be desirable at this point is its extension to three-dimensional media. Such an extension is expected to be quite straightforward since the numerical solution technique would be identical to that presently used. It would also completely generalize the medium properties available for investigation and would permit its broad application to sound propagation problems of many varieties. The method is not intended for supersonic flow rates, however. A further introduction of sound attenuation along a ray path would also permit atmospheric and undersea sound propagation studies with this method.

APPENDIX A

DESCRIPTION OF GEOMETRIC ACOUSTICS COMPUTER PROGRAM

A computer program was composed to carry out the numerical solution of the ray path equations derived in the text of this report. The program determines the propagation of a three-dimensional phase surface emanating from a stationary point source by following the path of a "bundle" of rays (a central and four surrounding rays) as they pass from a stationary point source through arbitrary two-dimensional flow and fluid property fields. These fields are treated as being continuous. The program also computes the average intensity and sound pressure for an acoustic-energy-conservative ray bundle at specific points along its path through the fluid medium. The program is applicable as a basic tool in evaluating measurements of sound which must propagate through an inhomogeneous medium before being received by the measuring microphone.

The specific situation envisaged for analysis is that of determining the sound radiation pattern of a point source located within an inhomogeneous moving medium as determined by a microphone at either a constant radius or side line position from an arbitrary point. Interaction of the microphone with any local flow is not accounted for since it is in a relatively quiescent region. Neither are discontinuous changes of fluid and flow properties considered, since these are approximations to real property variations and can be treated by simpler mathematical means.

In the following the program structure, operation and usage are described. Included are the input and output nomenclature, the input keypunch format and a listing of the program and current subroutines for the flow field and sound pressure level.

Main Program SART

This part of the program contains the input and output sections as well as sections for the calculation of the ray bundle size and step-size along the ray paths. It also calls the subroutines used in the programs to identify the reference condition for the subsequent sound pressure and intensity calculations (PIREF), to determine the local flow field proper-

ties (Mach number, speed of sound and density) involved in the calculations (FLOW), and to solve the differential equation of the ray path (YPPZPP).

The first action of SART is to read in the input data for the particular job. First is the HEADER card which describes within an 80 character space the job to be run. Next is a body of numerical information contained in a namelist group entitled INP. The specific items are described in figure A-1. This input information is then written out. Finally the source emission angles, ϕ_s and θ_s (degrees) for which the central ray path calculations are to be carried out are read in using the format indicated in figure A-2. Each value of ϕ_s is used with each value of θ_s up to the numbers NPHI and NTHETA (given in INP) in order as listed.

The angles and position information are then transformed to an internal coordinate system and converted (e.g. degrees to radians) where necessary. A compound DO loop is then entered to carry out the calculations for each combination of ϕ_s and θ_s.

The angles for the four bounding rays of the ray bundle are determined first. Then the initial flow field information is obtained by calling the subroutine FLOW.

Based on this flow field information the program then calls subroutine PIREF, which calculates the reference quantities necessary to determine the sound pressure level and sound intensity at susequent points along the path of the ray bundle.

The program then enters a section in which the paths of each ray in the bundle are calculated for the same step in time. In this manner, the positions of the rays at the end of each such step represents the intersection of the rays with a surface of constant phase. The position changes are determined using the direction cosines of the path, the fluid velocity and speed of sound, each evaluated at the starting position for the step.

The magnitude of the time step is determined by applying certain limiting criteria to the path of the central ray. Numerical values for these are input in the namelist INP. These criteria are:

1. The final distance, YYF (maximum radial or side line distance from a specified point (XXC, YYC, ZC)) shall not be passed.

Namelist INP

Column 2

XXC, YYC, ZC	Position of control point for constant radius calculation
XXØ, YYØ, ZØ	Initial position of source
NSL	0, calculations will end when YY-YYØ=YYF 1, calculations will end when the radial distance from (XXC, YYC, ZC) is YYF
YYF	Ray displacement for final calculation
AØ	Reference speed of sound
MØ	Mach number scale (e.g. maximum Mach number) for FLOW
RHØØ	Reference density
SIGMA	Scale parameter for shear layer. Used in FLOW
IAR	Reference energy emitted by source
MS	Provision for including source Mach number. Not presently used
DELPHI	Half angle of ray bundle in ϕ_s direction
DELTH	Half angle of ray bundle in θ_s direction
DELMIN	Minimum step size along ray path calculations
DVLIM	Maximum fractional change in velocity to be used
PF	Printout factor. Printout occurs if path length since last printout is greater than PF·DELT·AØ
MAX	Maximum number of steps allowed before reaching YYF
NPHI	Number of ϕ_s's to be used
NTHETA	Number of θ_s's to be used
$END	

Figure A-1 Namelist INP Format and Definitions

a) Input ϕ_s's (degrees):

Format (8F10.5) 8 values per card

column number	10	20	30	...	10NPHI
program variable	PHIØ(1)	PHIØ(2)	PHIØ(3)	...	PHIØ(NPHI)

b) Input θ_s's (degrees):

Format (8F10.5) 8 values per card

column number	10	20	30	...	10NPHI
program variable	TTØ(1)	TTØ(2)	TTØ(3)	...	TTØ(NTHETA)

Figure A-2 Wave Normal Angle Input Format

2. The step shall be such that the position of the central ray will change by an amount at <u>least</u> equal to DELMIN.
3. The time step shall be <u>no greater</u> than DELT.
4. The relative change in velocity $\Delta V/V$ over the step shall be no greater than DVLIM.

Of these criteria, the first three are absolute and the fourth governs only when they are not violated. Similarly, the first takes precedence over the second and third.

New direction cosines are obtained at the new position by calculation of their rates of change using the Euler-Lagrange equations developed in the text. The Euler-Lagrange equations are solved in the subroutine YPPZPP.

After completing this calculation for each of the five rays in the bundle, the program either repeats the calculation for the next time step or, if it is to print out information at this position, it proceeds to calculate the area of the ray bundle. The wavefront area, dA_p is approximated as follows. Consider the ray bundle depicted in the sketch below.

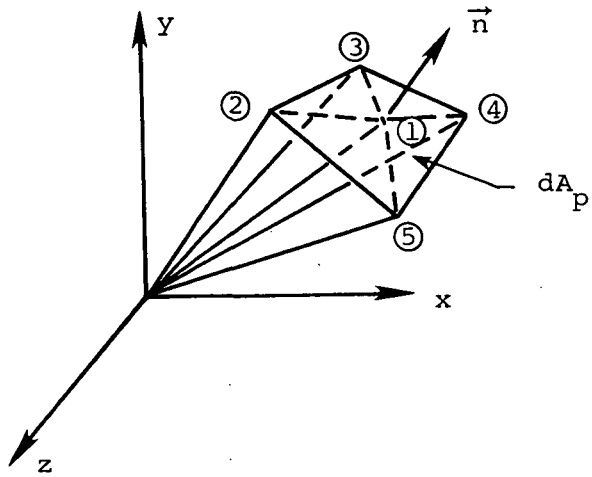

The area of a general triangle may be computed as follows

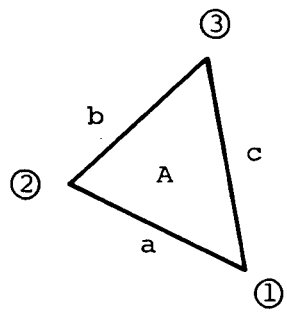

$$A = [S(S-a)(S-b)(S-c)]^{1/2}$$

$$S = \frac{1}{2}(a + b + c)$$

$$a = [(x_1-x_2)^2 + (y_1-y_2)^2 + (z_1-z_2)^2]^{1/2}$$

$$b = [(x_2-x_3)^2 + (y_2-y_3)^2 + (z_2-z_3)^2]^{1/2}$$

$$c = [(x_3-x_1)^2 + (y_3-y_1)^2 + (z_3-z_1)^2]^{1/2}$$

where the subscripted quantities are the Cartesian coordinates of the associated points ①, ②, ③, etc., the intersections of the correspondingly numbered rays with the phase surface.

The triangular sub-areas may be computed by this formula and dA_p then determined by summing the four sub-areas.

Note that all areas are positive and if there is a crossing of rays the method will break down and too low an intensity will be indicated.

If the final phase surface has been determined, that is, if the specified radial or side line distance, YYF, has been attained, the program additionally calculates the radius and center of curvature of the phase surface. This will enable the user to simply determine the sound intensity and pressure level at other positions along the ray path if the phase surface inside the bundle is in, and remains entirely in, a uniform medium. A definition of the output quantities appears in figure A-3.

The computations involved have assumed that $\partial/\partial z$ of any flow or fluid property is identically zero. This is the ONLY part of the program which restricts it to a two-dimensional fluid and flow field. Inclusion of the general z dependence terms in the derivatives will enable the treatment of a fully three-dimensional field. All acoustical propagation calculations presently consider the wave to be fully three-dimensional.

Subroutine FLOW

The subroutine FLOW provides the main program SART with flow and fluid property information at arbitrary positions along a ray path. The specific information to be provided is:

a) Output for ray position slope and flow field data

K	Ray number
XX YY ZZ	Spatial position
XXP	dXX/dYY for ray path
ZZP	dZZ/dYY for ray path
PHIE THETAE	Polar angles of wavenormal
MXX	Local flow Mach number in XX-direction
MYY	Local flow Mach number in YY-direction
A/AØ	Normalized speed of sound
RHØ/RHØØ	Normalized density

b) On first printout at initial position

REFERENCE INTENSITY = IAREF for direction of ray #1

c) Output for ray path length and polar position data

STEP NO.	Cumulative number of time steps
PATH LENGTH	Distance along path of ray #1
RADIAL DISPLACEMENT	Radial distance from source
GAMMA PSI	Polar angles of position from source
RØ	Distance traveled at speed, AØ, in elapsed time, Δt, i.e. AØ·Δt
RC	Radial distance from reference point (XXC,YYC,ZC)
GAMMAC PSIC	Polar angles of position relative to reference point

Figure A-3 Definition of Output Quantities

d) Output for acoustic intensity and sound pressure level

AN — Area of phase surface intercepted by ray bundle

IN — Acoustic intensity in direction of wave normal (IAREF/AN ~ energy flow per unit area)

DELTA SPL — Sound pressure level relative to a point source in a uniform flow field with conditions and properties being those at the source position and having the initial wave normal directions.

$$\sim \text{dB re } P_{ref}$$

where

$$P_{ref}(x,y,z) = \left.\frac{\rho a}{4\Delta\phi\Delta\theta(1 + M_n)^2}\right|_{(xo,yo,zo)} \cdot \frac{1}{(R(x,y,z)}$$

M_n = fluid velocity in wave normal direction/a

R = radial distance from source position (xo,yo,zo)

Figure A-3 Concluded

1. The density, RHO
2. The speed of sound, A
3. The vector Mach number, i.e., velocity vector/speed of sound
4. The spatial gradients of items 2 and 3

The main program presently accepts only two-dimensional fields. Hence, FLOW must provide RHO(x,y), A(x,y), MX(x,y), MY(x,y) and the partial derivatives of the latter three with respect to x and y. These are passed to SART via the argument list.

Provision is made in SART to pass certain information through a common block labeled FLUID. It has the form:

```
CØMMØN/FLUID/AØ,MØ,RHØØ,SIGMA,NWRITE
```

The quantities AØ, MØ and RHØØ may be used to normalize the speed of sound, Mach number and density, respectively, and are input in the namelist INP.

SIGMA may be used to scale the velocity gradient as in a self-similar flow where the velocity $u = u(\eta)$, where $\eta = \sigma y/s$. SIGMA or σ is also input through INP.

The quantity NWRITE permits the title or a description of the flow field to be written in the output whenever NWRITE is set equal to zero by the main program.

Subroutine PIREF

The subroutine PIREF is provided to calculate reference values for subsequent computation of sound pressure level and intensity in the main program. The required input data are:

a. The wave normal angles at the central ray, PHI and THETA.
b. The included half-angles of the ray bundle, DELPHI and DELTH.
c. The vector Mach number, MX and MY, at the source position.
d. The fluid density and speed of sound at the source position.
e. A reference energy, IAR, equal to the source energy (the product of phase surface area and intensity normal to that surface).

Items a, b, and c are input directly through the namelist INP. Items c and d are computed by FLØW at the initial source position.

The subroutine computes:

a. The Mach number in the direction of the initial wave normal, EMNØ.
b. The reference sound pressure, PREF, for a uniform flow having the properties of the fluid at the initial source position.
c. The reference energy, IAREF, in the direction of the given wave-normal.

The sample PIREF "computes" IAREF for a simple monopole source (i.e. IAREF=IAR) which has uniform emission in all directions. A higher order source, for example a dipole aligned with the x-axis ($\Phi = 90°$, $\theta = 0°$) may be represented by IAREF=IAR cos θ sin Φ and may be computed by thusly changing the defining statement for IAREF in PIREF.

The reference pressure need not be changed for other sources since the directional factors cancel out in the calculation of the sound pressure level.

Subroutine YPPZPP

The objective of subroutine YPPZPP is equivalent to determining the rates of change of the direction cosines of a ray given their values and that of the other flow properties and gradients indicated in the Euler-Lagrange equations.

The program does not actually deal with direction cosines but rather with the rates of change of two of the path spatial coordinates with the third taken as an independent variable. It should be noted that the computations are carried out in an internal system of coordinates in which the independent variable is "y" of the external coordinates (e.g. those used in FLOW) is identical to the internal "x". Where both coordinate systems appear in the program (e.g. the SART) we have adopted the notation:

EXTERNAL	INTERNAL
XX	-Y
YY	X (independent in YPPZPP)
ZZ	Z

As can be seen, this is a simple 90° rotation about the z-axis. The rotation was performed to better use the standard library trigonometric routines of the computer.

The major calculations of YPPZPP as is seen in the listing are concerned with the computation of various partial and total derivatives from the basic flow and fluid property information provided by FLOW.

PROGRAM LISTING

The program is written in FORTRAN IV computer language (029 punch) and consists of a main program, SART, and three subroutines. A listing of the program is given on the following pages.

```
      PROGRAM SART(INPUT,OUTPUT,TAPE5=INPUT,TAPE6=OUTPUT)
C
      REAL MX,MY,MX2,        MXX,MXXN,MYY,MYYN,MO,IAR,IAREF,IN
C
      COMMON/DERIV/ YPP,ZPP,MX,MY
      COMMON/FLOWC/ A,DADX,DADY,DMXDX,DMXDY,DMYDX,DMYDY
      COMMON/MAINC/G,M2,DENOM
      COMMON/FLUID/ AO,MO,RHOO,SIGMA,NWRITE
      COMMON/REF/ PREF,IAREF,IAR,DELPHI,DELTH,MXX,MYY,MS,AREF,RHOREF
C
      DIMENSION HEADER(8),PHIO(10),THETAO(10),TTO(10),DELX(5)
      DIMENSION X(5),Y(5),Z(5),YP(5),ZP(5),PHIK(5),THETAK(5)
      DIMENSION DYP(5),DZP(5)
C
      DATA DTOR/.0175329252/
      DATA PI/3.1415926535898/
      NAMELIST/DEBUG/YP,ZP,YPP,ZPP,RP,M2,        MX,MY
      NAMELIST/FLOWARG/ XX,YY,MXX,MYY,A,DADXX,DADYY,DMXXDXX,DMXXDYY,
     *   DMYYDXX,DMYYDYY
      NAMELIST/ANGL/ PHIO,THETAO,PHIK,THETAK,DELPHI,DELTH
      NAMELIST/INP/ XXC,YYC,ZC,XXO,YYO,ZO,NSL,YYF,AO,MO,RHOO,SIGMA,IAR,
     *MS,DELPHI,DELTH,DELT,DELMIN,DVLIM,PF,MAX,NPHI,NTHETA
C
 1000 FORMAT(11F10.5)
 1001 FORMAT(I5)
 1002 FORMAT(//10X,22HSOURCE POSITION, XXO =,F10.5,5X,5HYYO =,F10.5,5X,
     *5HZZO =,F10.5//10X,25HREFERENCE POSITION, XXC =,F10.5,5X,5HYYC =,F
     *10.5,5X,5HZZC =,F10.5//10X,29HAVE NORMAL DIRECTION, PHIE =,F10.5,
     *5X,8HTHETAE =,F10.5//10X,13HMACH NO, MO =,F10.5,5X,20HSPEED OF SOU
     *ND, AO =,F10.5,5X,15HDENSITY, RHOO =,E12.5//10X,32HREFERENCE ENERG
     *Y,IR*AR/RHOO**3 =,E12.5/)
 1013 FORMAT(10X,18HSTEP SIZE, DELS =,F10.5,5X,*DELTAPHI =*,F10.5,5X,
     **DELTA THETA =*,F10.5//)
 1102 FORMAT(10X,*MAXIMUM SIDE LINE POSITION, YYF =*,F10.5//)
 1113 FORMAT(10X,*MAXIMUM RADIUS, RF =*,F10.5//)
 1003 FORMAT(8A10)
 1004 FORMAT(5X,1HK,7X,2HXX,8X,2HYY,8X,2HZZ,7X,3HXXP,7X,3HZZP,
     *      4X,4HPHIS,6X,6HTHETAS,6X,3HMXX,7X,3HMYY,
     *      6X,4HA/AO,5X,8HRHO/RHOO/)
 1005 FORMAT(//* RAY HAS NOT REACHED SPECIFIED LIMIT WITHIN*,I5,* CALCUL
     *ATION STEPS*//)
 1006 FORMAT(8F10.5)
 1007 FORMAT(*1*)
 1008 FORMAT(1H1,8A10//)
 1009 FORMAT(1X,I5,11F10.5)
 1010 FORMAT(//1X,4HSTEP, 8X,4HPATH,11X,6HRADIAL/2X,3HNO.,  7X,6HLENGTH,
     *7X,12HDISPLACEMENT,6X,5HGAMMA,10X,3HPSI,13X,2HRO,14X,2HRC,11X,
     *6HGAMMAC, 9X,4HPSIC/)
 1011 FORMAT(I5,2(2(4X,E12.5),2(4X,F10.5)))
 1012 FORMAT(/* REFERENCE INTENSITY =*,E12.5,5X,*RHOO AO =*,E12.5,5X,
     *   12HRHOO AO)**2 =,E12.5,5X,12HRHOO AO)**3 =,E12.5/)
C
C
C
C READ INPUT
C
C
      READ(5,1003) HEADER
      READ(5,INP)
      WRITE(6,INP)
      WRITE(6,1008) HEADER
      IF(DELMIN.LT.1.E-6) GO TO 51
      READ(5,1006) (PHIO(I),I=1,NPHI)
      READ(5,1006) (TTO(I),I=1,NTHETA)
C
C TRANSFORM TO INTERNAL COORDINATE SYSTEM
C
      XO=YYO
      YO=-XXO
      XC=YYC
      YC=-XXC
C
      DTOR=PI/180.
      DO 5 I=1,NTHETA
    5 THETAO(I)=TTO(I)-90.0
C
C
C DO LOOPS FOR PHI AND THETA
C
      DO 50 I=1,NPHI
      DO 50 J=1,NTHETA
C
C        DEFINE INITIAL ANGLES FOR RAY TUBE
C            AND CONVERT TO RADIANS
C
      PHIK(1) = PHIO(I)*DTOR
      PHIK(2) = PHIK(1) -DELPHI *DTOR
      PHIK(3) = PHIK(2)
      PHIK(4) = PHIK(1) + DELPHI*DTOR
      PHIK(5) = PHIK(4)
      THETAK(1) = THETAO(J)*DTOR
      THETAK(2) = THETAK(1)-DELTH*DTOR
      THETAK(3) = THETAK(1)+DELTH*DTOR
      THETAK(4) = THETAK(3)
      THETAK(5) = THETAK(2)
C
C CALL FLOW FOR INITIAL FLOW CONDITIONS (FLOW SR USES EXTERNAL
C    COORDINATE SYSTEM)
      XX=XXO
      YY=YYO
C
      NWRITE=0
      CALL FLOW(XX,YY,MXX,MYY,A,DADXX,DADYY,DMXXDXX,DMXXDYY,DMYYDXX,
     *   DMYYDYY,RHO)
      NWRITE=1
      MY=-MXX
      MX=MYY
C
      DO 8 K=1,5
      X(K)=XO
      Y(K)=YO
      Z(K)=ZO
      PHIR=PHIK(K)
      THETAR=THETAK(K)
      SPHIR=SIN(PHIR)
      M2=SPHIR*COS(THETAR)
      M=MX+M2
      YP(K)= (MY+SPHIR*SIN(THETAR))/M
      ZP(K)= COS(PHIR)/M
    8 CONTINUE
```

```
C
      AREF=A
      RHOREF =RHO
      CALL PIREF(PHIO(I),TTO(J))
      DELS=AO*DELT
      RHAO =RHOO*AO
      RHAO2=RHAO*AO
      RHAO3=RHAO2*AO
      XF=YYF
      S=0.
      SPR=S
      RO=0.
      NPR=1
      NS=1
C
C WRITE HEADING FOR ONE SOUND RAY PATH TRACKING
C
      WRITE(6,1002) XXO,YYO,ZO,XXC,YYC,ZC,PHIO(I),TTO(J),MO,AO,RHOO,
     *IAREF
      WRITE(6,1013) DELS,DELPHI,DELTH
      IF(NSL.NE.0) GO TO 9
      WRITE(6,1113) XF
      GO TO 10
    9 CONTINUE
      WRITE(6,1102) XF
   10 CONTINUE
      IF(NS.GT.MAX) GO TO 48
      NS=NS+1
      DO 40 K=1,5
      XX=Y(K)
      YY=X(K)
      PHIR=PHIK(K)
      THETAR=THETAK(K)
      CALL FLO=(XX,YY,MXX,MYY,A,DADXX,DADYY,DMXXDXX,DMXXDYY,DMYYDXX,
     *   DMYYDYY,RHO)
      MY=MXX
      MX=MYY
      DADX=DADYY
      DADY=DADXX
      DMXDX=DMYYDYY
      DMXDY=DMYYDXX
      DMYDX=DMXXDYY
      DMYDY=DMXXDXX
C
      SPHIR=SIN(PHIR)
      H2=SPHIR*COS(THETAR)
      H=MX+H2
      G=A*H
C
C
C COMPUTE NEW PHI AND THETA
C
      MX2=MX*MX
      YP2=YP(K)**2
      ZP2=ZP(K)**2
      RP=1.+YP2+ZP2
      T100=1.0+YP2
      T102=YP(K)*MX+MY
      T103=T100*MX-YP(K)*T102
      PHIR= ACOS((ZP(K)/RP)*(T103
     *   +SQRT((RP*(T100-T102**2)-ZP2*T103**2)/T100)))
      SPHIR=SIN(PHIR)
      SPHIR2=SPHIR**2
      THETAR=ASIN((T102+YP(K)*SQRT(T100*SPHIR2-T102**2))/(T100*SPHIR))
      PHIK(K)=PHIR
      THETAK(K)=THETAR
C
C
C     COMPUTE DELX,YPP AND ZPP
C
      GDLS=G*DELS
      IF(K.NE.1) GO TO 20
      EMN=SPHIR*(MX*COS(THETAR)+MY*SIN(THETAR))
C
C        COMPUTE DISTANCE AND DIRECTION FROM SOURCE
C
      DX=X(1)-XO
      DY=Y(1)-YO
      DZ=Z(1)-ZO
      R=SQRT(DX*DX+DY*DY+DZ*DZ)
      DXC=X(1)-XC
      DYC=Y(1)-YC
      DZC=Z(1)-ZC
      RC=SQRT(DXC**2+DYC**2+DZC**2)
      IF(NS.EQ.0) GO TO 14
      RO=RDT*DELS+RO
      GAMR=ACOS(DZ/R)
      PSIR=ACOS(DX/(R*SIN(GAMR)))
      IF(DY.LT.0.) PSIR=-PSIR
      GAM=GAMR/DTOR
      PSI=PSIR/DTOR
      PSIE=PSI+90.
      GAMCR=ACOS(DZC/RC)
      PSICR=ACOS(DXC/(RC*SIN(GAMCR)))
      IF(DYC.LT.0.) PSICR=-PSICR
      GAMC=GAMCR/DTOR
      PSIC=PSICR/DTOR+90.
   14 CONTINUE
      RDT=1.
      RHOA1=RHO*A
      RHOA3=RHO*A**3
      VGRAD=ABS(  DMXXDYY/MO)
      VGR=VGRAD*GDLS/DVLIM
      IF(VGR.GT.1.) RDT=1.0/VGR
      DEL=RDT*GDLS
      IF(DEL.GT.GDLS) RDT=1.
      IF(DEL.LT.DELMIN)  RDT=DELMIN/GDLS
      DEL=RDT*GDLS
      XN=X(1)+DEL
      YN=Y(1)+DEL*YP(1)
      ZN=Z(1)+DEL*ZP(1)
C        SET UP + CALL FLO=
      XXN=YN
      YYN=XN
      CALL FLO=(XXN,YYN,MXXN,MYYN,AN,DNA,DNB,DNC,DND,DNE,DNF,DNG)
      DELM=ABS(  (MXXN-MXX)/MO)
      IF(DELM.GT.DVLIM) RDT=RDT*DVLIM/DELM
      DEL=RDT*GDLS
      IF(DEL.LT.DELMIN) RDT=DELMIN/GDLS
      DEL=RDT*GDLS
```

```
      XN=X(1)+DEL
C
C         CONSTANT RADIUS CALCULATION
C
      IF(NSL.NE.0) GO TO 19
      YN=Y(1)+DEL*YP(1)
      ZN=Z(1)+DEL*ZP(1)
      RP=SQRT((XC-XC)**2+(YN-YC)**2+(ZN-ZC)**2)
      DRP=DXC+YP(1)*DYC+ZP(1)*DZC
      IF(RN.GT.XF) RDT=(-DRP+SQRT(DRP**2+(XF**2-RC**2)*RP))/(RP*GDLS)
      SN=RC
      GO TO 17
C
C         CONSTANT SIDE LINE CALCULATION
C
   15 CONTINUE
      IF(XN.GT.XF)     RDT =  (XF-X(1))/(XN-X(1))
      SN=X(1)
   17 CONTINUE
C
      IF(S-SPR.GE.PF*DELS) SPR=S
      IF(SPR.EQ.S) NPR=1
      IF(SN.GE.XF) NPR=1
      IF(NPR.EQ.0) GO TO 19
      IF(NS.EQ.0) GO TO 18
      WRITE(6,1010)
      WRITE(6,1011) NS,S,R,GAM,PSIE,RO,RC,GAMC,PSIC
   18 CONTINUE
C WRITE COLUMN HEADINGS
      WRITE(6,1004)
C
   19 CONTINUE
      DELX(1)=RDT*GDLS
      S=S+DELX(1)*SQRT(RP)
   20 CONTINUE
      DELA(K)=RDT*GDLS
C
C
      YPP=0.
      ZPP=0.
      CALL YPPZPP(YP(K),ZP(K))
      DYP(K)=YPP
      DZP(K)=ZPP
      IF(NPR.EQ.0) GO TO 23
C
C         SKIP IF NPR=0
C
      PHID=PHIR/DTOR
      THETAD=THETAR/DTOR
C
C TRANSFORM TO EXTERNAL COORDINATE SYSTEM
C
      TTE=THETAD+90.0
      XX=Y(K)
      YY=X(K)
      ZZ=Z(K)
      XXP=YP(K)
      ZZP=ZP(K)
      WRITE(6,1009) K,XX,YY,ZZ,XXP,ZZP,PHID,TTE,MXX,MYY,A,RHO
C
      IF(K.NE.5) GO TO 23
      IF(NS.EQ.0) GO TO 22
C
C         COMPUTE AREA OF PHASE SURFACE WITHIN RAY TUBE
C
      SA2= SQRT((X(1)-X(2))**2+(Y(1)-Y(2))**2+(Z(1)-Z(2))**2)
      SA3= SQRT((X(1)-X(3))**2+(Y(1)-Y(3))**2+(Z(1)-Z(3))**2)
      SA4= SQRT((X(1)-X(4))**2+(Y(1)-Y(4))**2+(Z(1)-Z(4))**2)
      SA5= SQRT((X(1)-X(5))**2+(Y(1)-Y(5))**2+(Z(1)-Z(5))**2)
      SB = SQRT((X(2)-X(3))**2+(Y(2)-Y(3))**2+(Z(2)-Z(3))**2)
      SC = SQRT((X(4)-X(3))**2+(Y(4)-Y(3))**2+(Z(4)-Z(3))**2)
      SD = SQRT((X(4)-X(5))**2+(Y(4)-Y(5))**2+(Z(4)-Z(5))**2)
      SE = SQRT((X(2)-X(5))**2+(Y(2)-Y(5))**2+(Z(2)-Z(5))**2)
      SAB= 0.5*(SA2+SB+SA3)
      SAC= 0.5*(SA4+SC+SA3)
      SAD= 0.5*(SA4+SD+SA5)
      SAE= 0.5*(SA2+SE+SA5)
      AB= SQRT(SAB*(SAB-SA2)*(SAB-SB)*(SAB-SA3))
      AC= SQRT(SAC*(SAC-SA3)*(SAC-SC)*(SAC-SA4))
      AD= SQRT(SAD*(SAD-SA4)*(SAD-SD)*(SAD-SA5))
      AE= SQRT(SAE*(SAE-SA5)*(SAE-SE)*(SAE-SA2))
      AN=AB+AC+AD+AE
C
C         COMPUTE  INTENSITY NORMAL TO PHASE SURFACE
C         IAREF IS THE ENERGY EMITTED FROM THE SOURCE INTO THE RAY TUBE
C
      IN=IAREF/AN
C
C         COMPUTE THE SOUND PRESSURE LEVEL RE A REFERENCE SOURCE
C
      PREF2=PREF/RO**2
      PRAR2= RHOA1/(PREF2*AN*(1.+EMN)**2)
      SPL=10.*ALOG10(PRAR2)
      WRITE(6,1020)  AN,IN,SPL
 1020 FORMAT(10X,*AN = *,2X,E12.5,5X,*IN =  *,E12.5,5X,*DELTA SPL =  *,
     * F10.5//)
      IF(ABS(SN-XF).LE.1.E-6) GO TO 40
      GO TO 23
   22 CONTINUE
      WRITE(6,1012) IAREF,RHOA,RHOA2,RHOA3
   23 CONTINUE
   40 CONTINUE
      NPR=0
      IF(MAX-NB.LT.2) NPR=1
C
C     COMPUTE NEW POSITION,YP AND ZP.
C
      DO 47 K=1,5
      X(K)=X(K)+DELX(K)
      Y(K)=Y(K)+YP(K)*DELX(K)
      Z(K)=Z(K)+ZP(K)*DELX(K)
      YP(K)=YP(K)+DYP(K)*DELX(K)
      ZP(K)=ZP(K)+DZP(K)*DELX(K)
   47 CONTINUE
      GO TO 10
   48 CONTINUE
      WRITE(6,1005) NS
C
C    COMPUTE  CENTER OF CURVATURE AND RADIUS OF CURVATURE OF PHASE
C         SURFACE AT FINAL STATION
```

```
C
   49 CONTINUE
      DAY=YP(2)-YP(4)
      DAZ=ZP(2)-ZP(4)
      CY2=Y(2)-YP(2)*X(2)
      CY4=Y(4)-YP(4)*X(4)
      CZ4=Z(4)-ZP(4)*X(4)
      CZ2=Z(2)-ZP(2)*X(2)
      YA=(CY4*YP(2)-CY2*YP(4))/DAY
      ZA=(CZ4*ZP(2)-CZ2*ZP(4))/DAZ
      XA=(CY4-CY2)/DAY
      RA=SQRT((XA-X(2))**2+(YA-Y(2))**2+(ZA-Z(2))**2)
      YYA=XA
      XXA=-YA
      WRITE(6,1030) XXA,YYA,ZA,RA
 1030 FORMAT(/10X,*THE CENTER OF CURVATURE OF THE FINAL PHASE SURFACE IS
     * AT XX = *,F10.5/67X,*YY = *,F10.5/67X,*ZZ = *,F10.5/
     *10X,*THE RADIUS OF CURVATURE IS *,F10.5//)
      WRITE(6,1007)
C
   50 CONTINUE
      GO TO 52
   51 WRITE(6,1021)
 1021 FORMAT(* STEP SIZE NOT CORRECTLY INPUT.*)
   52 CONTINUE
      STOP
      END


      SUBROUTINE YPPZPP(YP,ZP)
C
      REAL MX,MY,MX2,MXP,MY2
C
      COMMON/DERIV/ YPP,ZPP,MX,MY
      COMMON/MAINC/G,M2,DENOM
      COMMON/FLDAC/ A,DADX,DADY,DMXDX,DMXDY,DMYDX,DMYDY
C
      NAMELIST/DEBUG/ M2,A1,A2,DM1,DM2,DM4,DM5,DM14,DM15,DM24,DM25,DM44,
     *   DM45,DM54,DM55,T1,T2,T3,T4,T5,T6,T7,T8,T9,T10,T11,T12,CX,CY,CZ,
     *   D1,E1,E2,DENOM,F1,F2,DMXDX,DMXDY,MXP,DMYDX,DMYDY,TWOZP,DA1DZP,
     *DA2DZP
C
      YP2=YP*YP
      ZP2=ZP*ZP
      YP2ZP2=YP2+ZP2
      RP=1.0+YP2ZP2
      RP2=RP*RP
      TWOYP=2.0*YP
      TWOZP=2.0*ZP
      S1=1.0+ZP2
      MX2=MX*MX
      S2=1.0-MX2
      MY2=MY*MY
      S3=(MY-2.0*YP*MX)
      A2= RP+TWOYP*MX*MY-YP2ZP2*MX2-S1*MY2
      S4=SQRT(A2)
      S5=S4**3
      S6=2.0*S4
      S7=4.0*S5
      RPINV=1/RP
      S8=TWOYP/RP
      S9=TWOZP/RP
C
C DERIVATIVES OF A1
C
      DA1DX=YP2ZP2*DMXDX-YP*DMYDX
      DA1DY=YP2ZP2*DMXDY-YP*DMYDY
      DA1DYP=TWOYP*MX-MY
      DA1DZP=TWOZP*MX
C
C LET T1=DDX(DA1DYP)
C
      T1=TWOYP*DMXDX-DMYDX
C
C LET T2=DDY(DA1DYP)
C
      T2=TWOYP*DMXDY-DMYDY
C
C LET T3=DDX(DA1DZP)
C
      T3=TWOZP*DMXDX
C
C LET T4=DDY(DA1DZP)
C
      T4=TWOZP*DMXDY
C
C LET T5=DDYP(DA1DYP)
C
      T5=2.0*MX
C
C LET T6=DDZP(DA1DZP)
C
      T6=2.0*MX
C
C
C DERIVATIVES OF A2
C
C
      DA2DX=  2.0*((YP*MY-YP2ZP2*MX)*DMXDX+(YP*MX-S1*MY)*DMYDX)
      DA2DY=  2.0*((YP*MY-YP2ZP2*MX)*DMXDY+(YP*MX-S1*MY)*DMYDY)
      DA2DYP=2.0*(YP*S2+MX*MY)
      DA2DZP=TWOZP*(S2-MY2)
C
C LET T7=DDX(DA2DYP)
C
      T7=2.0*(S3*DMXDX+MX*DMYDX)
C
C LET T8=DDY(DA2DYP)
C
      T8=2.0*(S3*DMXDY+MX*DMYDY)
C
C LET T9=DDX(DA2DZP)
C
      T9=-4.0*ZP*(MX*DMXDX+MY*DMYDX)
C
C LET T10=DDY(DA2DZP)
C
      T10=-4.0*ZP*(MX*DMXDY+MY*DMYDY)
C
C LET T11=DDYP(DA2DYP)
C
      T11=2.0*S2
```

```
C
C LET T12=DDZP(DA2DZP)
C
      T12=2.0*(S2-MY2)
C
C
C DERIVATIVES OF M2
C
C     ADOPT DERIVATIVE SUBSCRIPT NOTATION ASSOCIATING 1 WITH X
C                                                     2 WITH Y
C                                                     4 WITH Y*
C                                                     5 WITH Z*
C
C
      DM2=(-DA1DY+DA2DY/S6)/RP
      DM1=(-DA1DX+DA2DX/S6)/RP
      DM4=(-T4*DYP*M2-DA1DYP+DA2DYP/S6)/RP
      DM5=(-T4*DZP*M2-DA1DZP+DA2DZP/S6)/RP
      DM14=(-T4*DYP*DM1-T1+T7/S6-DA2DX*DA2DYP/S7)/RP
      DM24=(-T4*DYP*DM2-T2+T8/S6-DA2DY*DA2DYP/S7)/RP
      DM44 = -2.*S6*DM4+(-2.*M2-T5+T11/S6-(DA2DYP**2)/S7)*RPINV
      DM45 = -S8*DM5-S9*DM4-DA2DYP*DA2DZP/(S7*RP)
      DM15=-S9*DM1+RPINV*(-T3+T9/S6-DA2DX*DA2DZP/S7)
      DM25=-S9*DM2+RPINV*(-T4+T10/S6-DA2DY*DA2DZP/S7)
      DM55 = -2.*S9*DM5+(-2.*M2-T6+T12/S6-(DA2DZP**2)/S7)*RPINV
C
C
C CALCULATION OF D1,E1,E2
C
C
      AP=(DADX*YP+DADY)/A
      AX=DM4
      AY=DM5
      CX=DM1+YP*DM2
C
      AY=  DM44
      HY=  DM45
      CY=AP*AX+  (DM14+YP*DM24)
C
      AZ=AY
      BZ=  DM55
      CZ=AP*AY+  (DM15+YP*DM25)
C
      M=MX+M2
      D1=AY-2.*AX*AX/M
      E1=BY-2.*AX*BX/M
      E2=BZ-2.*AY*BY/M
      DENOM=D1*E2-E1*E1
C
C TEST DENOM
C
      IF(ABS(DENOM).LT.1.E-06) GO TO 999
      MXP=DMXDX+YP*DMXDY
      F1=M*DADY/A+DMXDY+DM2+2.*AX*(AP+(MXP+CX)/M)-CY
      F2=2.*BX*(AP+(MXP+CX)/M)-CZ
      YPP=(F1*E2-F2*E1)/DENOM
      ZPP=(F2*D1-F1*E1)/DENOM
      RETURN
  999 WRITE(6,1000) DENOM
 1000 FORMAT(/,1X,8HDENOM = ,F10.5)
      RETURN
      END
```

```
      SUBROUTINE FLOW(X,Y,MX,MY,A,DADX,DADY,DMXDX,DMXDY,DMYDX,DMYDY,RHO)
C
      REAL M,MX,MY,MO
C
      COMMON/FLUID/ AO,MO,RHOO,SIGMA,NWRITE
      DATA B/1./,C/0./
C
C             SELF SIMILAR HYPERBOLIC TANGENT FLOW FIELD
C                  U = 0.5*(1.0)*(1+TANH Z )
C
C    A= SPEED OF SOUND/AO
C    RHO= DENSITY/RHOO
C    B= THE Y ORIGIN OF THE SHEAR LAYER
C    C= THE X ORIGIN OF THE SHEAR LAYER
C
 1000 FORMAT(10X,*HYPERBOLIC TANGENT FLOW FIELD, U=0.5(1+TANH(ETA))*//)
      IF(NWRITE.EQ.0) WRITE(6,1000)
      A=1.0
      RHO=1.0
      M=0.5*MO
      DADX=0.
      DADY=0.
      ABEX=ABS(X-C)
      ZETA=SIGMA*(B-Y)/ABEX
      IF(ABS(ZETA).GT.0.) GO TO 10
      TN=TANH(ZETA)
      TN2=TN*TN
      MX=M*(1.+TN)
      DZDY=SIGMA/ABEX
      DZDX=-ZETA/ABEX
      DMX=M*(1.-TN2)
       DMXDX=DMX*DZDX
      DMXDY=DMX*DZDY
      MY=(M/SIGMA)*(ZETA*TN+0.5*ALOG(1.-TN2) -ALOG(2.))
      DMYDX=DMXDY
      DMYDX=(M/SIGMA)*ZETA*(1.-TN2)*DZDX
      RETURN
   10 IF(ZETA.LT.0.) GO TO 20
      MX=M+2.0
      GO TO 25
   20 MX=0.
   25 MY=0.
      DMYDX=0.
      DMYDY=0.
      DMXDX=0.
      DMXDY=0.
      RETURN
      END
```

```
      SUBROUTINE PIREF(PHI,THETA)
      REAL IAR,IAREF,MX,MY,MS
      COMMON/REF/ PREF,IAREF,IAR,DELPHI,DELTH,MX ,MY ,MS,A,RHO
      DATA DTOR/.0175329252/
 1000 FORMAT(10X,*REFERENCE SOURCE IS A STATIONARY POINT SOURCE IN A UNI
     *FORMLY MOVING FLUID*/10X,*ALL REFERENCE FLOW PROPERTIES ARE EVALUA
     *TED AT THE INITIAL SOURCE POSITION*//)
      WRITE(6,1000)
      PHIR=PHI*DTOR
      THR=THETA*DTOR
      CT=COS(THR)
      ST=SIN(THR)
      SP=SIN(PHIR)
      DARD=4.*   DELPHI*DELTH*DTOR**2
      EMNO=SP*(MX*CT+MY*ST)
C
C        MONOPOLE SOURCE
C
      IAREF=IAR
      PREF=A*RHO/(DARD*(1.+EMNO)**2)
      RETURN
      END
```

APPENDIX B

VARIATION OF FLUID PROPERTIES

Much experimental work in low speed flows involve negligible variation of the fluid properties which affect sound propagation, specifically the density, ρ, and the speed of sound, a. In a compressible medium where high subsonic Mach numbers are involved, significant changes in these properties occur through regions of substantial velocity changes. In a constant pressure flow field with unity Prandtl number, as is normally assumed for a free subsonic jet, these properties are related to the velocity by the Crocco relation and the equation of state. The Crocco relation exists between the velocity and temperature of a perfect gas of constant specific heat, unity Prandtl number and at constant pressure, and is:

$$T = A + Bu - \frac{u^2}{2c_p} \tag{B.1}$$

where

T = the static temperature of the fluid

u = the velocity

c_p = the specific heat at constant pressure (assumed to be constant)

A,B = coefficients determined by the boundary conditions

If we let the subscripts j and ∞ indicate properties in the unmixed jet and the external medium, respectively, the conditions to be satisfied by equation (B.1) are

$$T_j = A + B\,u_j - \frac{u_j^2}{2c_p}$$

$$T_\infty = A + B\,u_\infty - \frac{u_\infty^2}{2c_p}$$

Upon using these conditions to evaluate the coefficients A and B, equation (B.1) becomes:

$$\frac{T}{T_j} = 1 - \frac{1-r}{1-\lambda}\left(1 - \frac{u}{u_j}\right) + \frac{\gamma-1}{2} M_j^2 \left[(1+\lambda)\frac{u}{u_j} - \lambda - \left(\frac{u}{u_j}\right)^2\right] \tag{B.2}$$

where

$r = T_\infty / T_j$

$\lambda = u_\infty / u_j$

$M_j = u_j / a_j$, the jet Mach number

γ = ratio of constant pressure and constant volume specific heats

a = speed of sound = $(\gamma RT)^{1/2}$

R = gas constant

For constant pressure flow of a perfect gas, the density and speed of sound variations with velocity may be computed using equation (B.2).

$$\frac{\rho}{\rho_j} = \frac{T_j}{T} \tag{B.3}$$

$$\frac{a}{a_j} = \left(\frac{T}{T_j}\right)^{1/2} \tag{B.4}$$

Thus, by specifying the velocity field and boundary conditions, all necessary properties of the medium can be determined.

APPENDIX C

ACOUSTIC INTENSITY AND SOUND PRESSURE LEVEL FOLLOWING A RAY BUNDLE

Along a ray path (with no absorption or generation) conservation of energy within a ray bundle requires that (see ref. 26)

$$\vec{I} \cdot \vec{n} dA = \text{const.} \tag{C.1}$$

where

$\vec{I}$ = acoustic intensity = the acoustic energy flux vector

dA = wave front area enclosed by the ray "bundle" or "tube"

$\vec{n}$ = normal to the wave front (i.e., the surface of constant phase)

In terms of physical quantities, $\vec{I}$ may be computed from the relation (see ref. 26)

$$\vec{I} = \left\langle p'\vec{u} + \frac{\vec{U}}{\rho_o a_o^2} p^2 + \frac{\vec{U}(\vec{U} \cdot \vec{u})}{a_o^2} p + \rho_o \vec{u}(\vec{U} \cdot \vec{u}) \right\rangle \tag{C.2}$$

where

a_o = speed of sound in the fluid

ρ_o = mean fluid density

p' = acoustic pressure

$\vec{U}$ = mean fluid velocity

$\vec{u}$ = acoustic particle velocity relative to the fluid

In the far field limit (i.e. $a/\omega r \to 0$) of geometric acoustics

$$\vec{u} \approx u_n \vec{e}_n \tag{C.3}$$

$$p' \approx \rho_o a_o u_n \tag{C.4}$$

where

$\vec{e}_n$ = unit vector in the wave normal direction

u_n = component of u in the $\vec{e}_n$ direction

The far field intensity in a direction $\vec{e}_R$ is

$$I_R = \vec{I} \cdot \vec{e}_R = \frac{\langle p'^2 \rangle}{\rho_o a_o} (1 + \vec{M} \cdot \vec{e}_n)(\vec{e}_n \cdot \vec{e}_R + \vec{M} \cdot \vec{e}_R) \tag{C.5}$$

where

$$\vec{M} = \vec{U}/a_o \tag{C.6}$$

If $\vec{e}_R = \vec{e}_n$, the wave normal direction

$$I_n = \frac{\langle p'^2 \rangle}{\rho_o a_o} (1 + \vec{M} \cdot \vec{e}_n)^2 \tag{C.7}$$

These relations hold in the geometric acoustics approximation, regardless of the type of source.

APPENDIX D

MOVING SOURCES

The motion of an ideal source of sound relative to an observer (microphone) introduces the so-called Doppler effects on the frequency, intensity, and directivity of the sound received from the source. The motion of a real source of finite dimensions relative to the fluid medium can additionally introduce changes in the basic character of the source (e.g. create additional monopole-, dipole-, and/or quadrupole-like noise issuing from the real source). Such changes cannot yet be concisely described but have their roots in the full Kirchhoff solution to the wave equation and the boundary conditions on the actual source. The discussion here will be restricted to a presentation of the Doppler effects for sources moving with respect to an observer. The basic Doppler effects for subsonic motion may be described as follows.

Consider a two-dimensional source moving at a uniform speed, V, relative to an observer at $0(x,y,z,t)$ as indicated in figure D-1. Sound received at time, t, from direction θ_s was emitted from the source at time $t - R_c/a_\infty$ and at a convected emission angle of θ_c. The convected emission angle is related to the actual emission angle, θ_s, and the fluid flow velocity as given previously by the ray path equations. Reduced to two dimensions, these yield

$$\tan \theta_c = \frac{v + a \sin \theta_s}{u + a \cos \theta_s} \tag{D.1}$$

where u, v, and a are the fluid velocities in the x and y directions and the local speed of sound at the point of emission, respectively.

The frequency, ω, of the sound received relative to that produced by the source, ω_o, may also be calculated

$$\omega = \frac{\omega_o}{1 + \dfrac{u_s \cos \theta_c + v_s \sin \theta_c}{a}} \tag{D.2}$$

where u_s and v_s are the x and y components, respectively, of the source velocity at the time of emission.

The energy received at point 0 from sources moving along a prescribed path may be determined by examining the energy reaching the point from various specific points along the path. The energy density received from each point may be determined from the ray path method as though the source were instantaneously stationary and in proportion to the emission of the source in the appropriate wave normal direction to intercept the point 0 from the source position. The energy from different points, of course, is emitted from the source at different times and would, therefore, yield a time history of energy received from the source as it travels along its given path with a prescribed velocity history and directivity.

Consider now a statistically stationary field of moving sources as one has with the noise produced by turbulence from a "steady" jet or wake. The noise associated with such flows is identified with convected quadrupoles. However, any given region of space involved in the flow has a characteristic strength, directivity, and spectrum which do not vary substantially with time. Given the directivity, strength, convection speed (essentially that of the flow), and the spectral nature of such sources in the flow, their characteristics may be modified to those of equivalent stationary sources by the above means [equations (D.1) and (D.2)]. The acoustical energy density (intensity) produced by the field point, 0, may then be determined as an appropriately weighted sum of that arriving from a number of representative points in the flow.

Three-dimensional versions of equations (D.1) and (D.2) may be obtained by using appropriate velocity components in the directions of the wave normal and ray path, respectively, instead of using the trigonometric functions indicated.

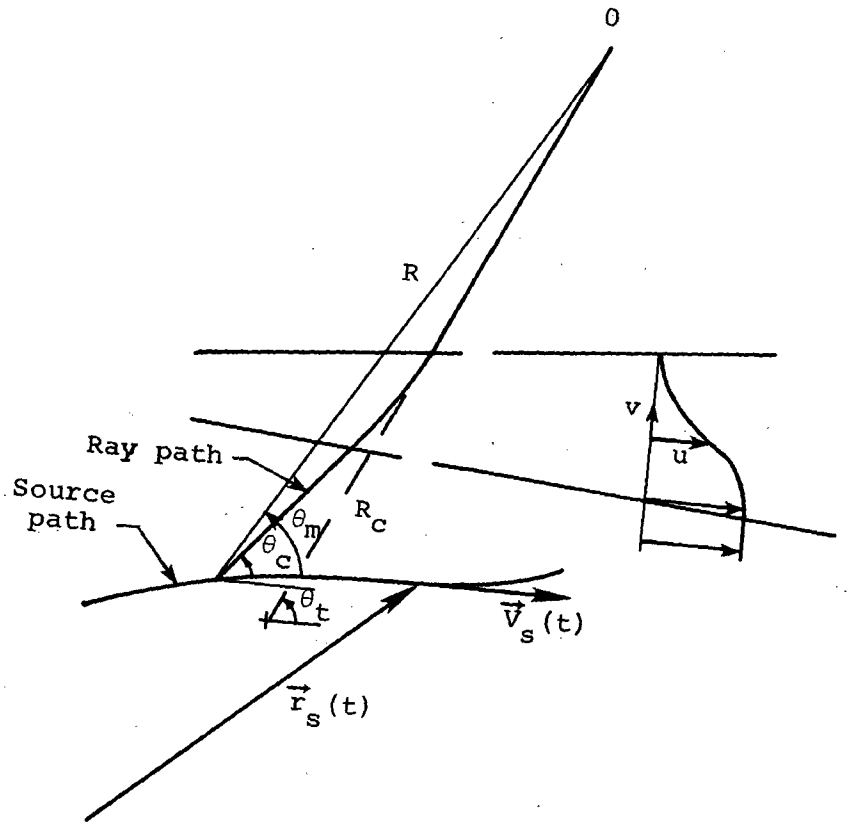

Figure D-1.- Moving source configuration.

REFERENCES

1. Woolley, J. P., Karamcheti, K., and Mendenhall, M. R.: The Design of an Anechoic Open-throat Wind Tunnel. Nielsen Engineering & Research, Inc. TR-66. Prepared under NASA Contract NAS2-7120, 1974.
2. Plumblee, H. E., ed.: Effects of Forward Velocity on Turbulent Jet Mixing Noise. NASA CR-2702, 1976.
3. Amiet, R. K.: Refraction of Sound by a Shear Layer. AIAA 15th Aerospace Sciences Meeting, Los Angeles, Jan. 24-26, 1977. AIAA Paper No. 77-54.
4. Gunzburger, M. D. and Kleinstein, G. G.: On the Mathematical Conditions for the Existence of Periodic Fluctuations in Nonuniform Media. J. Sound and Vib., Vol. 48, No. 3, 1976, pp. 345-357.
5. Blokhintsev, D. I.: Acoustics of a Nonhomogeneous Moving Medium. NACA TM-1399, 1956.
6. Schubert, L. K.: Refraction of Sound by a Jet: A Numerical Study. UTIAS Rept No. 144, Dec. 1969.
7. Lighthill, M. J.: On sound Generated Aerodynamically. II. Turbulence as a Source of Sound. Proc. Roy. Soc. London A, Vol. 222, pp. 1-32, 1954.
8. Phillips, O. M.: On the Generation of Sound by Supersonic Turbulent Shear Layers. J. Fluid Mech., Vol. 9, 1960, pp. 1-28.
9. Csanady, G. T.: The Effect of Mean Velocity Variations on Jet Noise. J. Fluid Mech., Vol. 26, Pt. 1, 1966, pp. 183-197.
10. Lilley, G. M.: Generation of Sound in a Mixing Region. AFAPL-TR-72-53, Vol. IV, 1972, pp. 2-97.
11. Doak, P. E.: On the Interdependence Between Acoustic and Turbulent Fluctuating Motions in a Moving Fluid. J. Sound and Vib., Vol. 19, Pt. 2, 1971, pp. 211-225.
12. Howe, M. S.: Contributions to the Theory of Aerodynamic Sound, with Application to Excess Jet Noise and the Theory of the Flute. J. Fluid Mech., Vol. 71, Pt. 4, 1975, pp. 625-673.
13. Yates, J. E. and Sandri, G.: Bernoulli Enthalpy: A Fundamental Concept in the Theory of Sound. 2nd Aeroacoustics Conf., Hampton, Virginia, Mar. 1975. AIAA Paper 75-439, 1975.
14. Balsa, T. F.: The Far Field of High Frequency Convected Singularities in Sheared Flows, with an Application to Jet-Noise Prediction. J. Fluid Mech., Vol. 74, Pt. 2, 1976, pp. 193-208.

15. Tester, B. J. and Morfey, C. L.: Developments in Jet Noise Modeling. Theoretical Predictions and Comparisons with Measured Data. 2nd Aeroacoustics Conf., Hampton, Virginia, Mar. 1975. AIAA Paper 75-477, also J. Sound and Vib., Vol. 46, 1975.
16. Atvars, J., Schubert, L. K., Grande, E., and Ribner, H. S.: Refraction of Sound by Jet Flow or Jet Temperature. NASA CR-494, 1966.
17. Grande, E.: Refraction of Sound by Jet Flow and Jet Temperature. NASA CR-840, 1967.
18. Dowling, A.: Convective Amplification of Real Simple Sources. J. Fluid Mech., Vol. 74, Pt. 3, 1976, pp. 529-546, 1976.
19. Ugincius, P.: Ray Acoustics and Fermat's Principle in a Moving Inhomogeneous Medium. J. Acous. Soc. of Am., Vol. 51, No. 5, Pt. 2, 1972, pp. 1,759-1,763.
20. Amiet, R. K.: Correction of Open Jet Wind Tunnel Measurements for Shear Lyaer Refraction. Progress in Astronautics and Aeronautics, Vol. 46, ed. I. R. Schwartz, pp. 259-280, 1976. 2nd Aeroacoustics Conf., Hampton, Virginia, Mar. 1975. AIAA Paper No. 75-532, 1975.
21. Jacques, J. R.: Noise from Moving Aircraft: Some Relevant Models. Ph.D Thesis, Cambridge University, 1975.
22. Ribner, H. S.: Reflection, Transmission, and Amplification of Sound by a Moving Medium. J. Acous. Soc. of Am., Vol. 29, No. 4, 1957, pp. 435-441.
23. Koutsoyannis, S. P.: Features of Sound Propagation Through and Stability of a Finite Shear Layer. TR-5, Joint Inst. for Aeronautics and Acoustics, Stanford University, 1977.
24. Mani, R.: The Influence of Jet Flow on Jet Noise. J. Fluid Mech., Vol. 73, Pt. 4, 1976, pp. 753-793.
25. Tester, B. J. and Burrin, R. H.: On Sound Radiation from Sources in Parallel Sheared Jet Flows. AIAA Paper 74-57, 1974.
26. Morfey, C. L.: Acoustic Energy in Non-Uniform Flows. J. Sound and Vib., Vol. 14, No. 2, 1971, pp. 159-170.

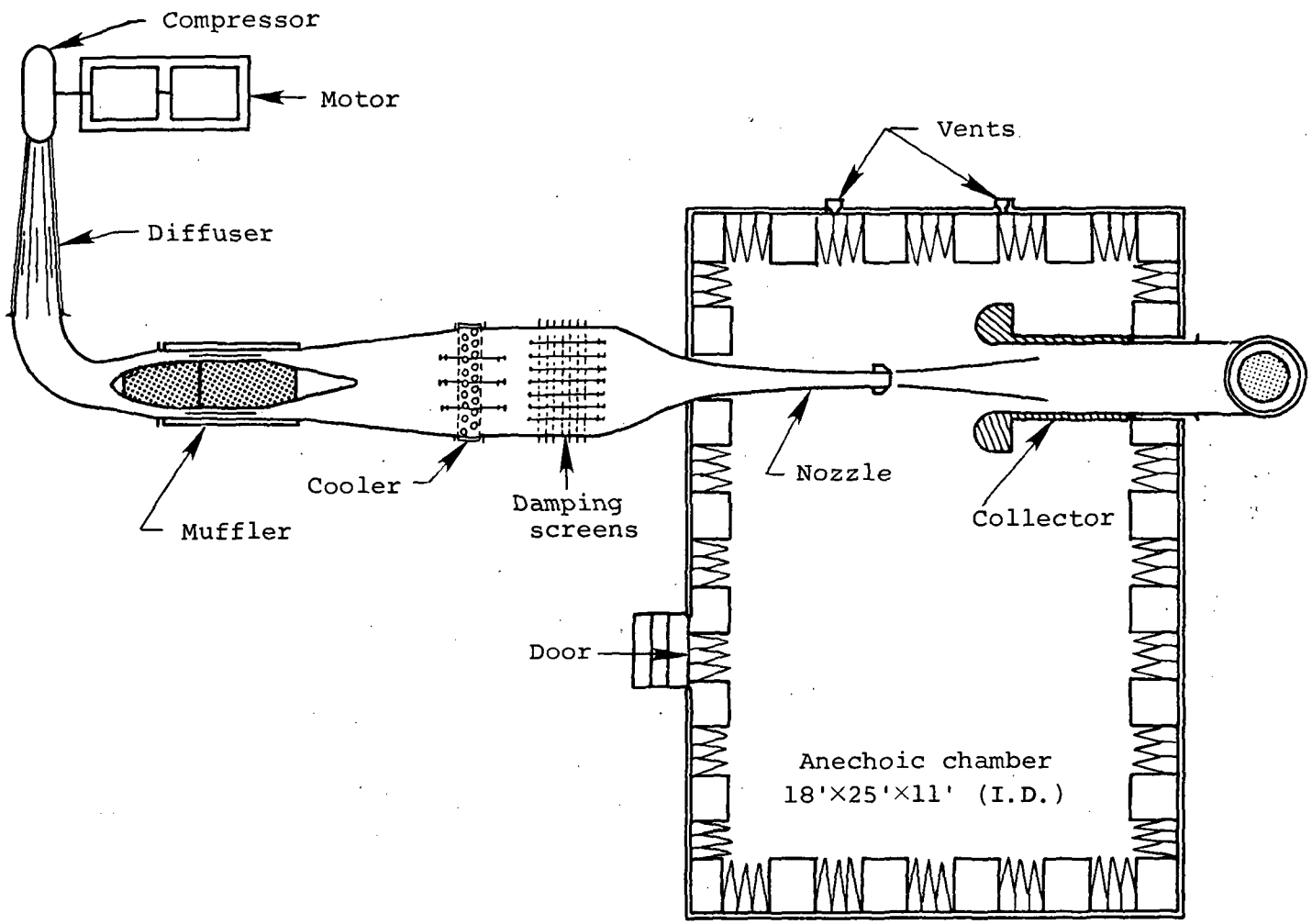

Figure 1.- General arrangement of anechoic open-throat wind tunnel.

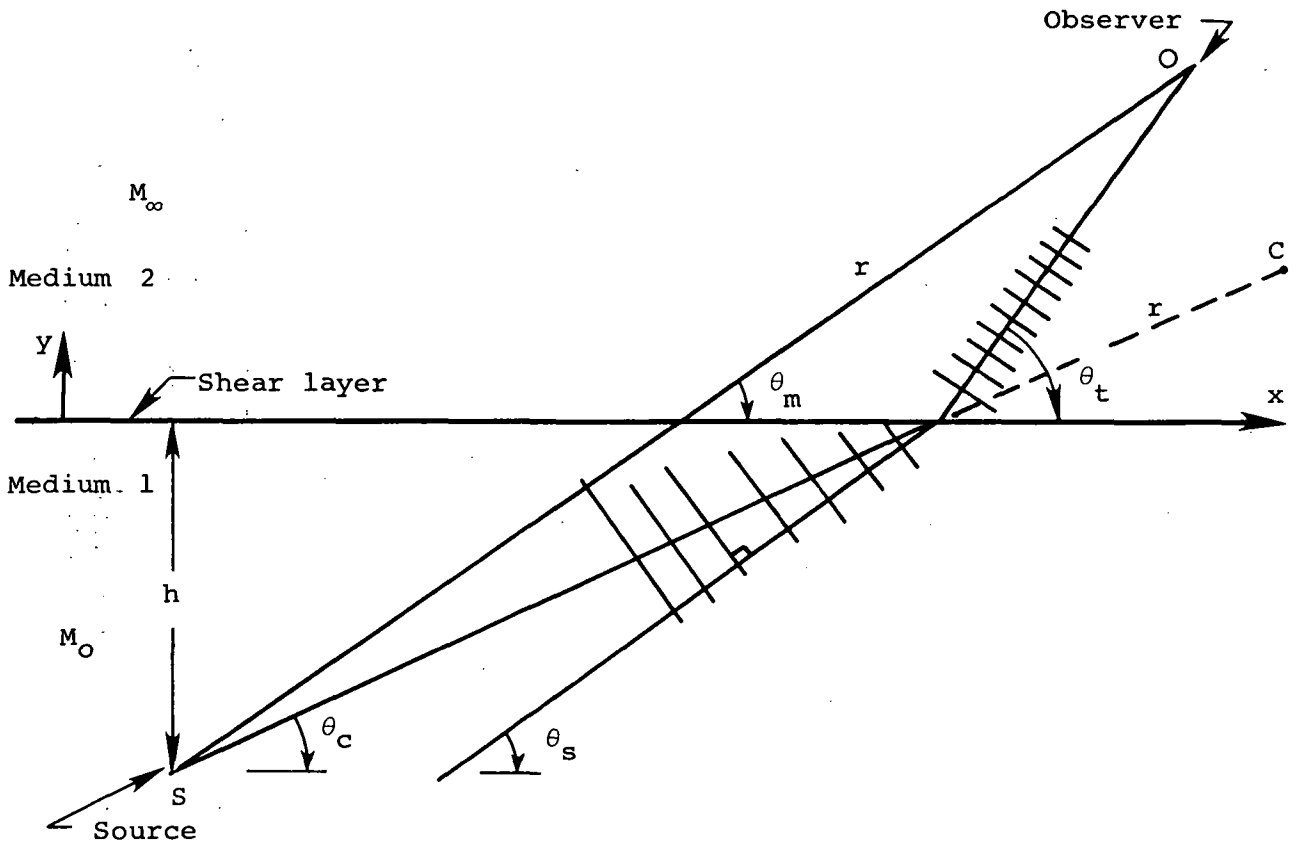

Figure 2.- Vortex sheet model of sound propagation through a shear layer.

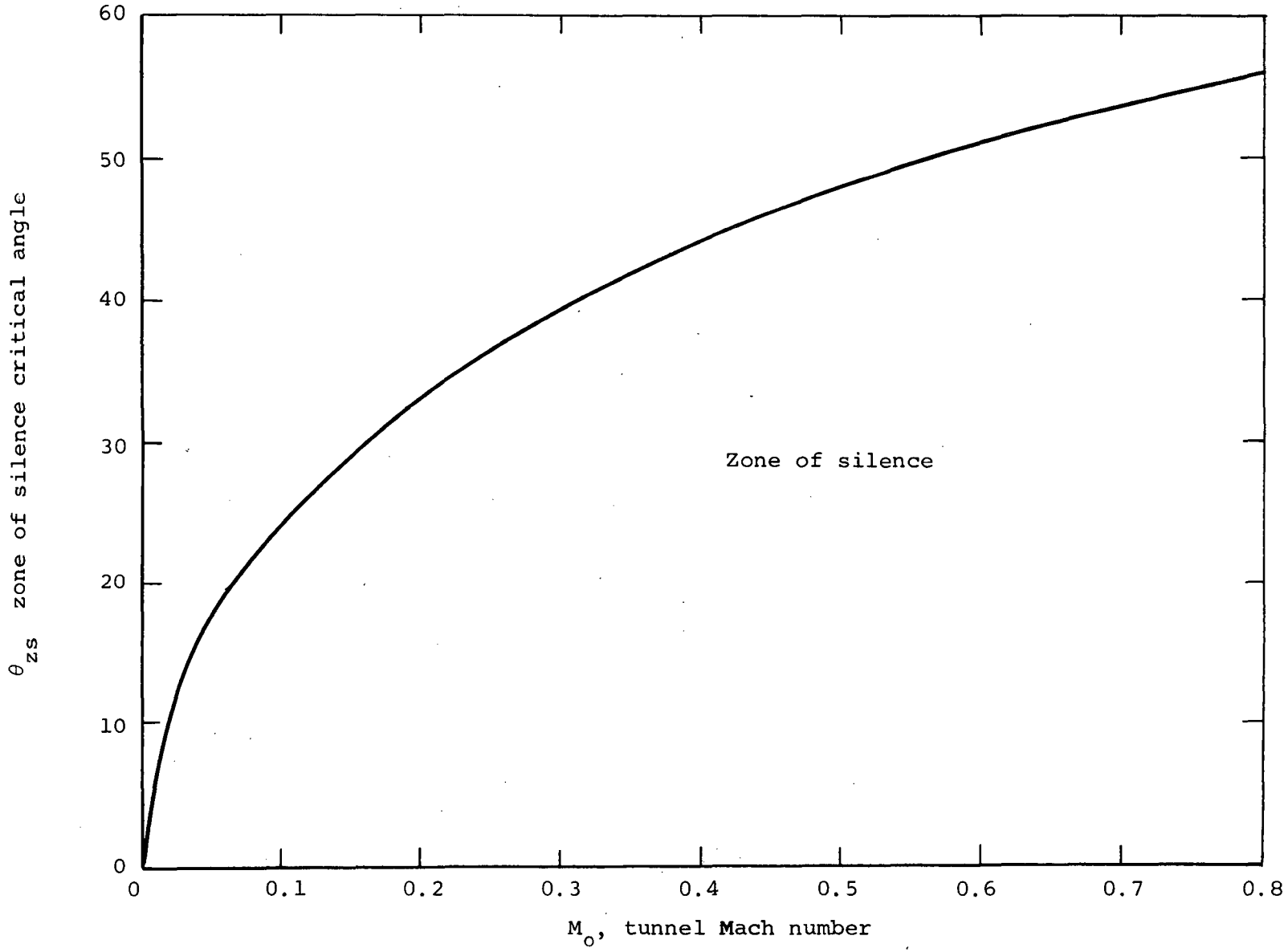

Figure 3.- Zone of silence critical angle versus tunnel Mach number for a plane vortex sheet shear layer.

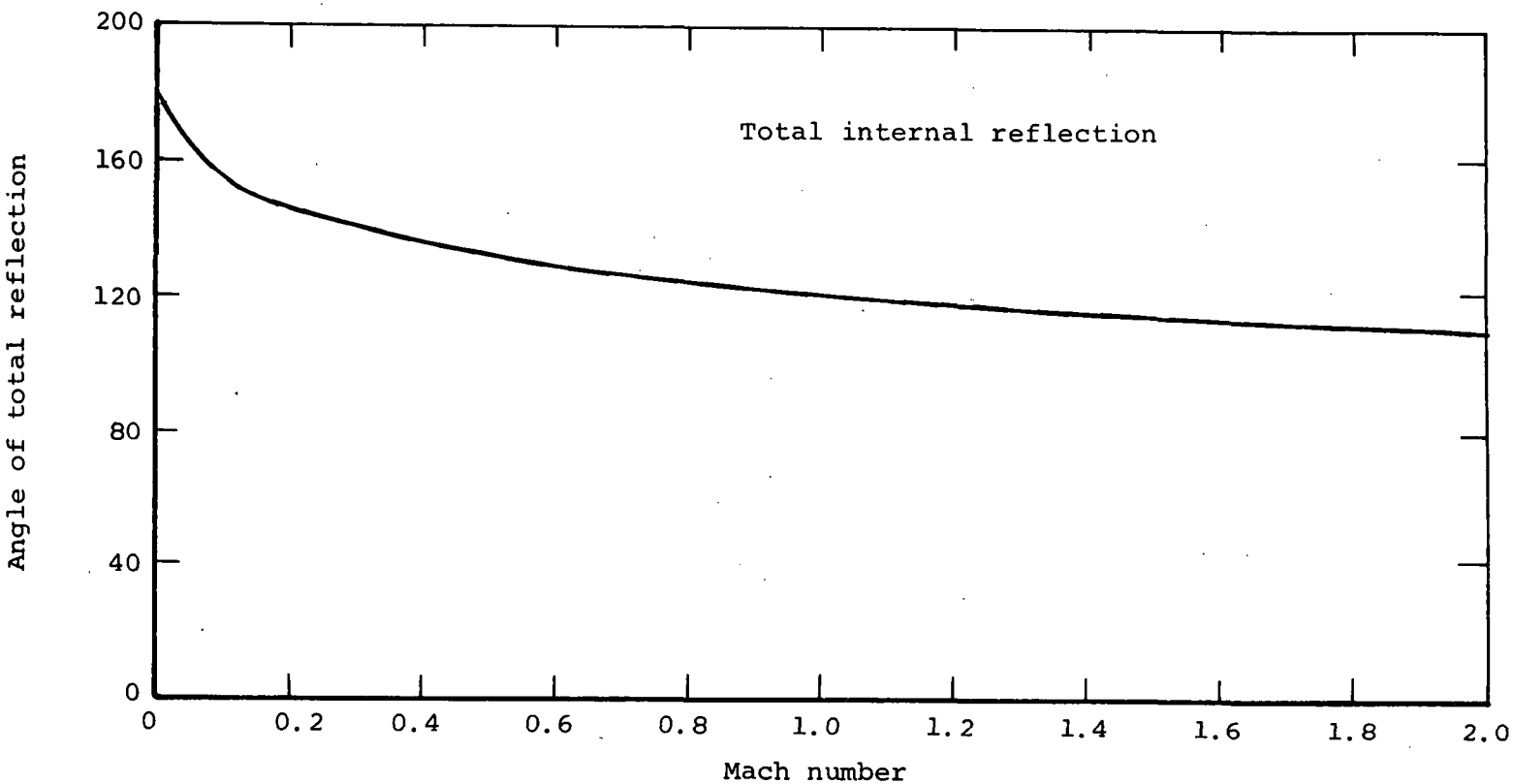

Figure 4.- Angle of total internal reflection versus tunnel Mach number for a plane vortex sheet shear layer.

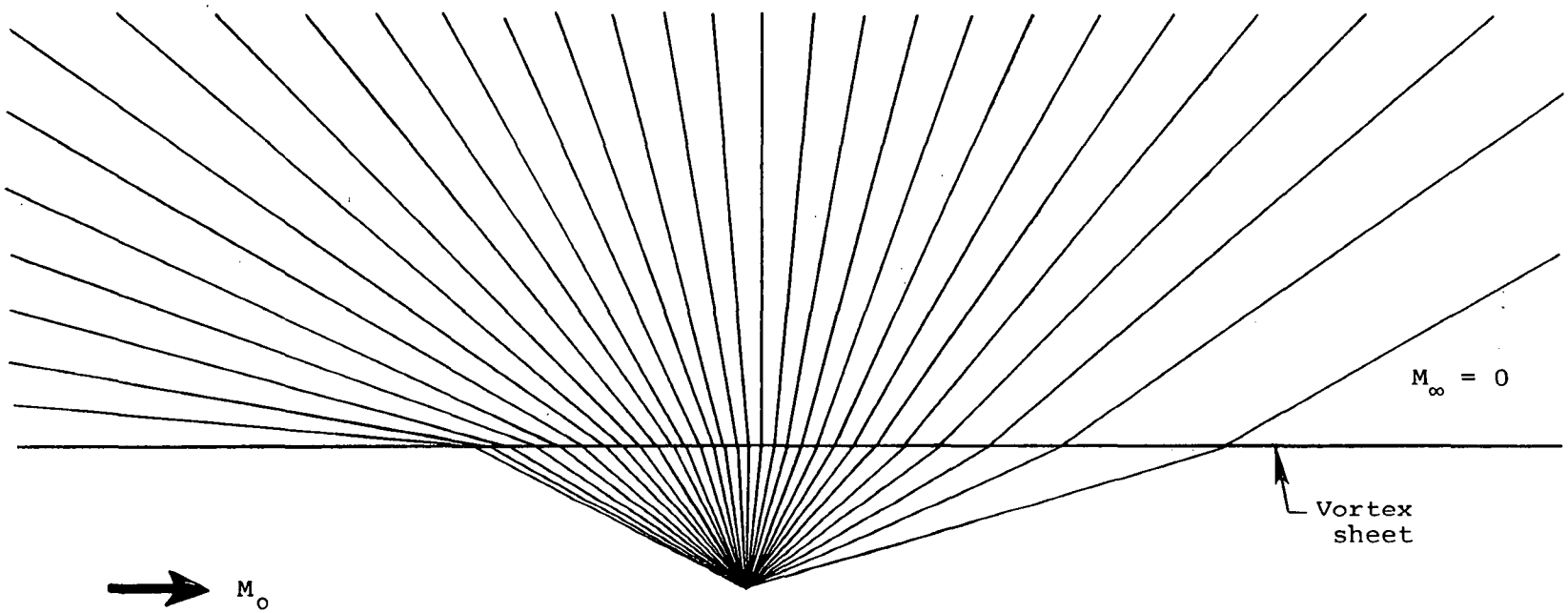

(a) $M_o = 0.1$.

Figure 5.- Directivity pattern, vortex sheet model.

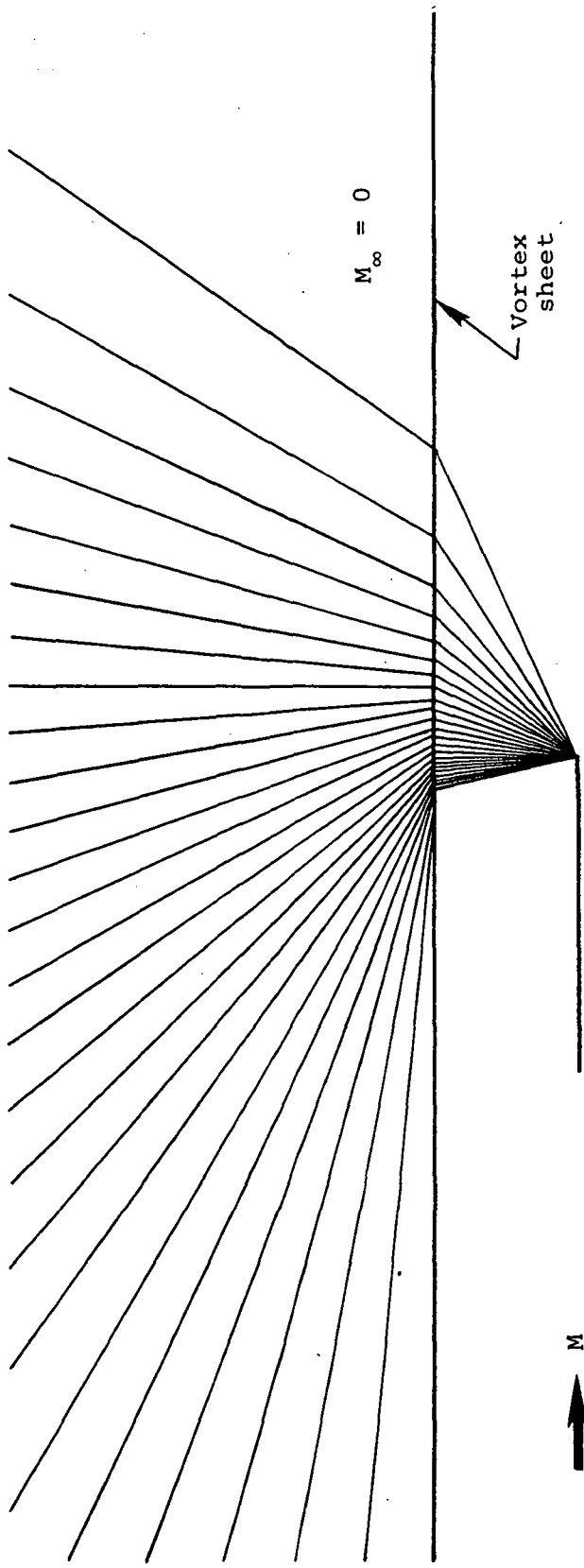

(b) $M_o = 0.5$.

Figure 5.- Continued.

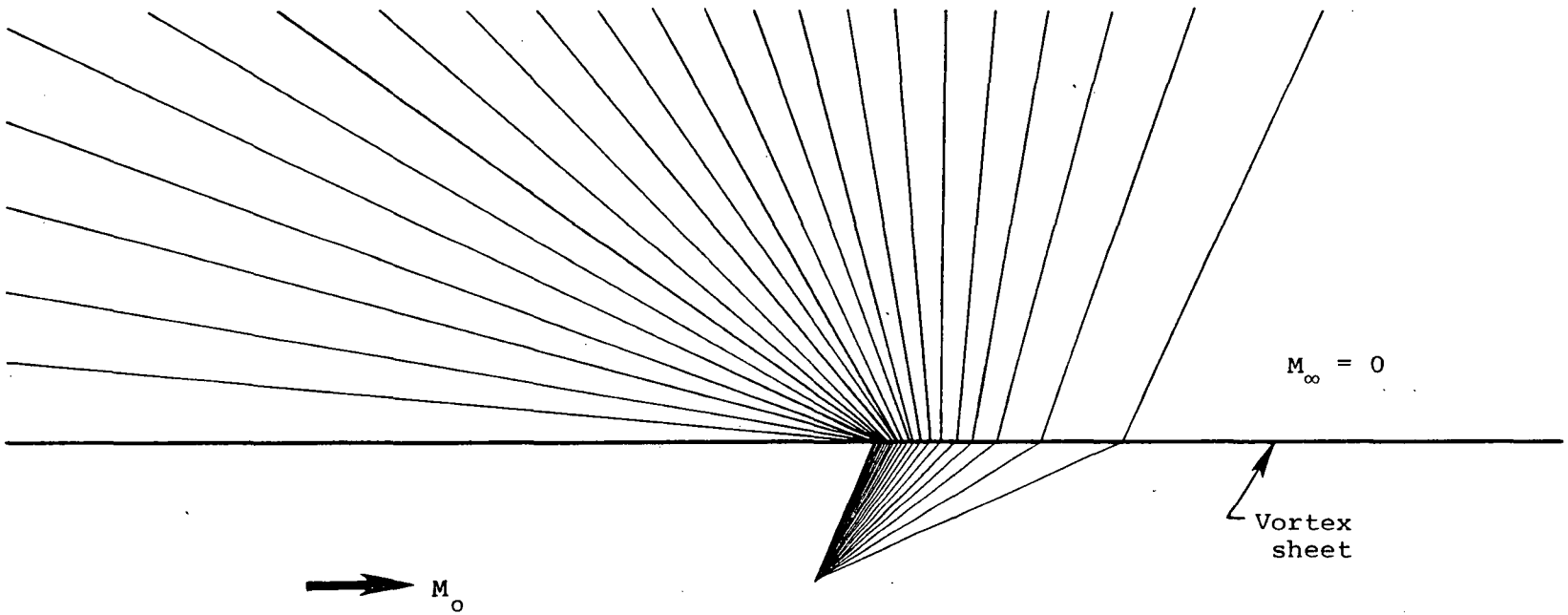

(c) $M_o = 0.9$.

Figure 5.- Concluded.

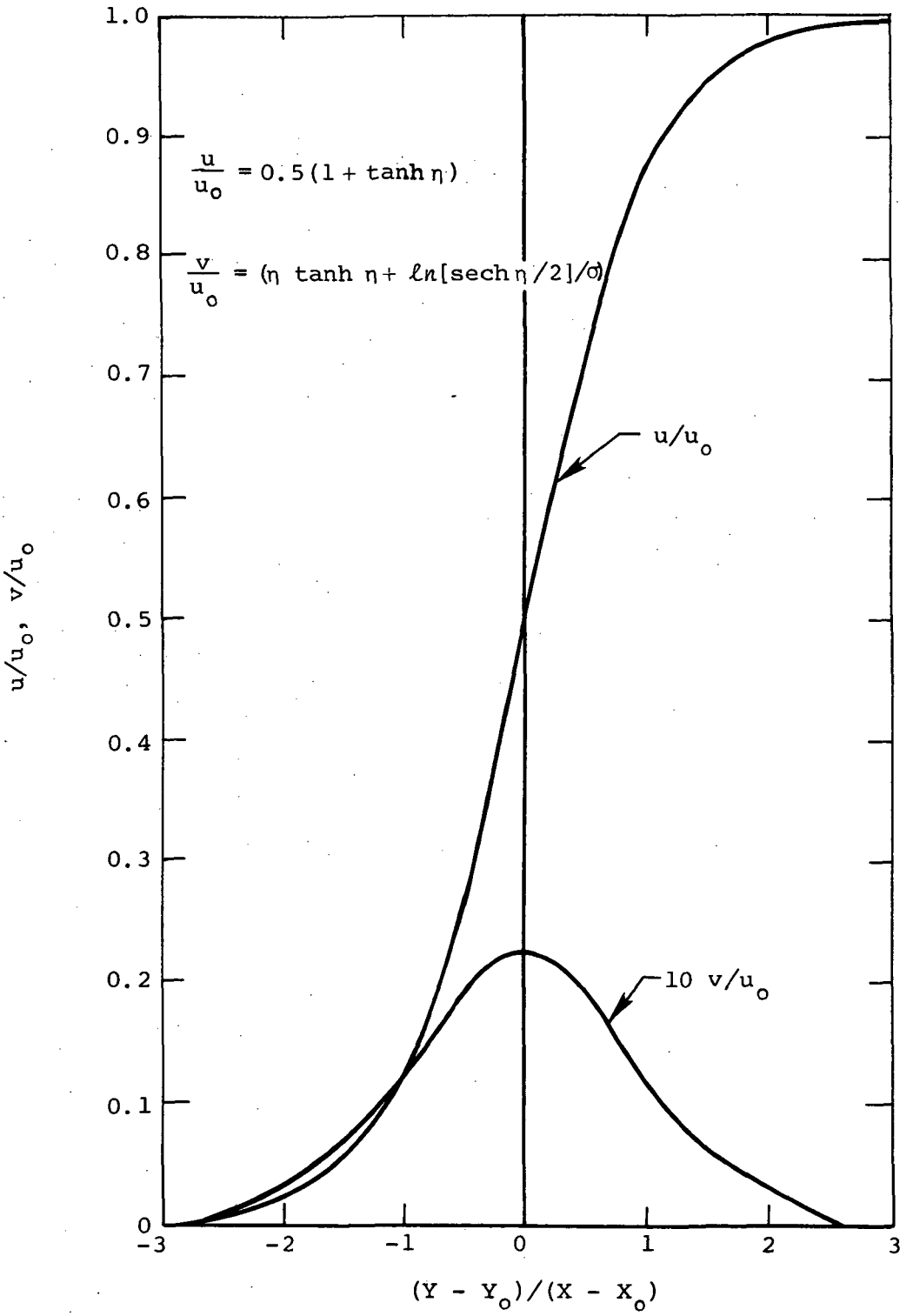

Figure 6.- Velocity profile used in analysis.

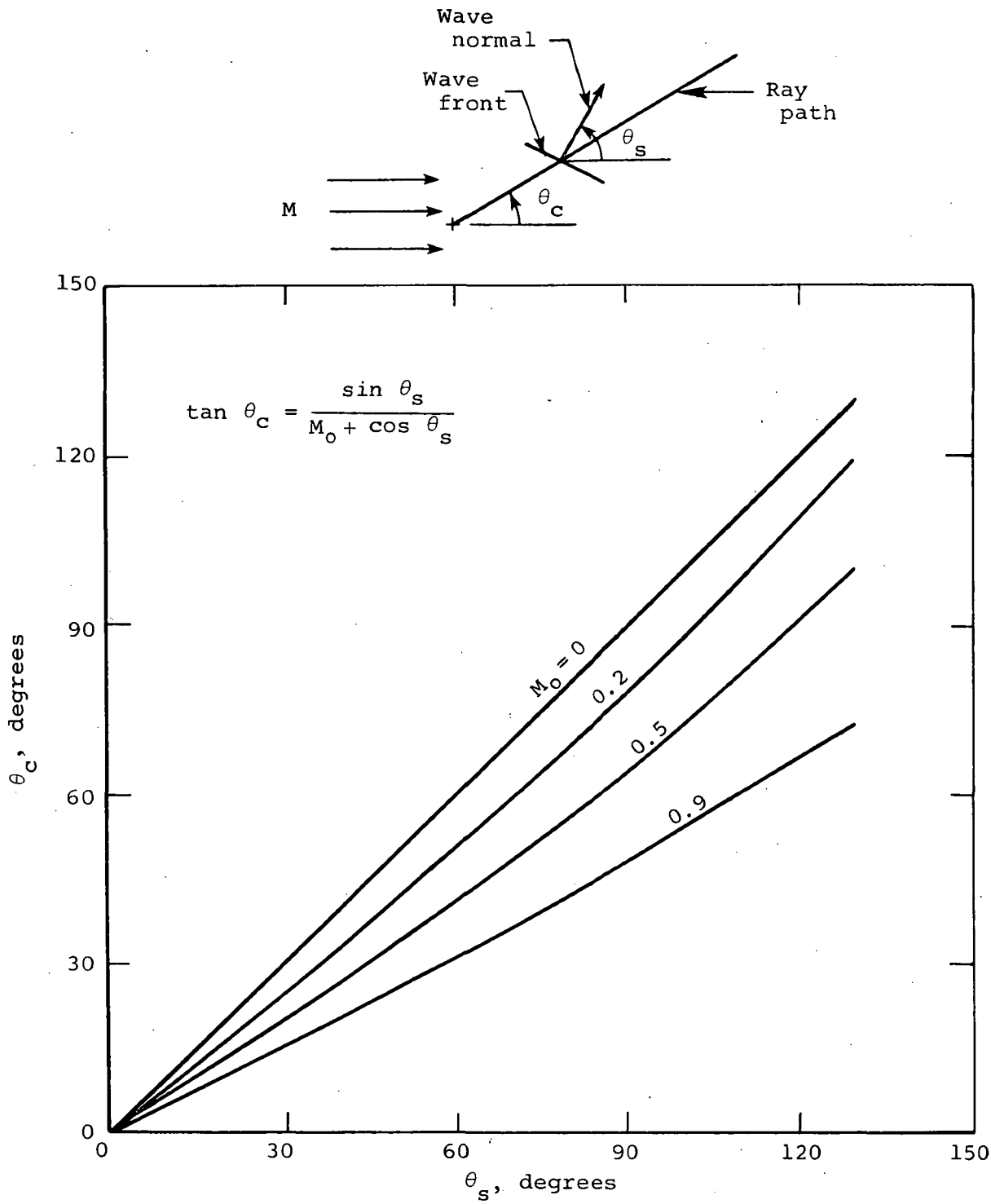

Figure 7.- Convected angle of ray path in parallel flow.

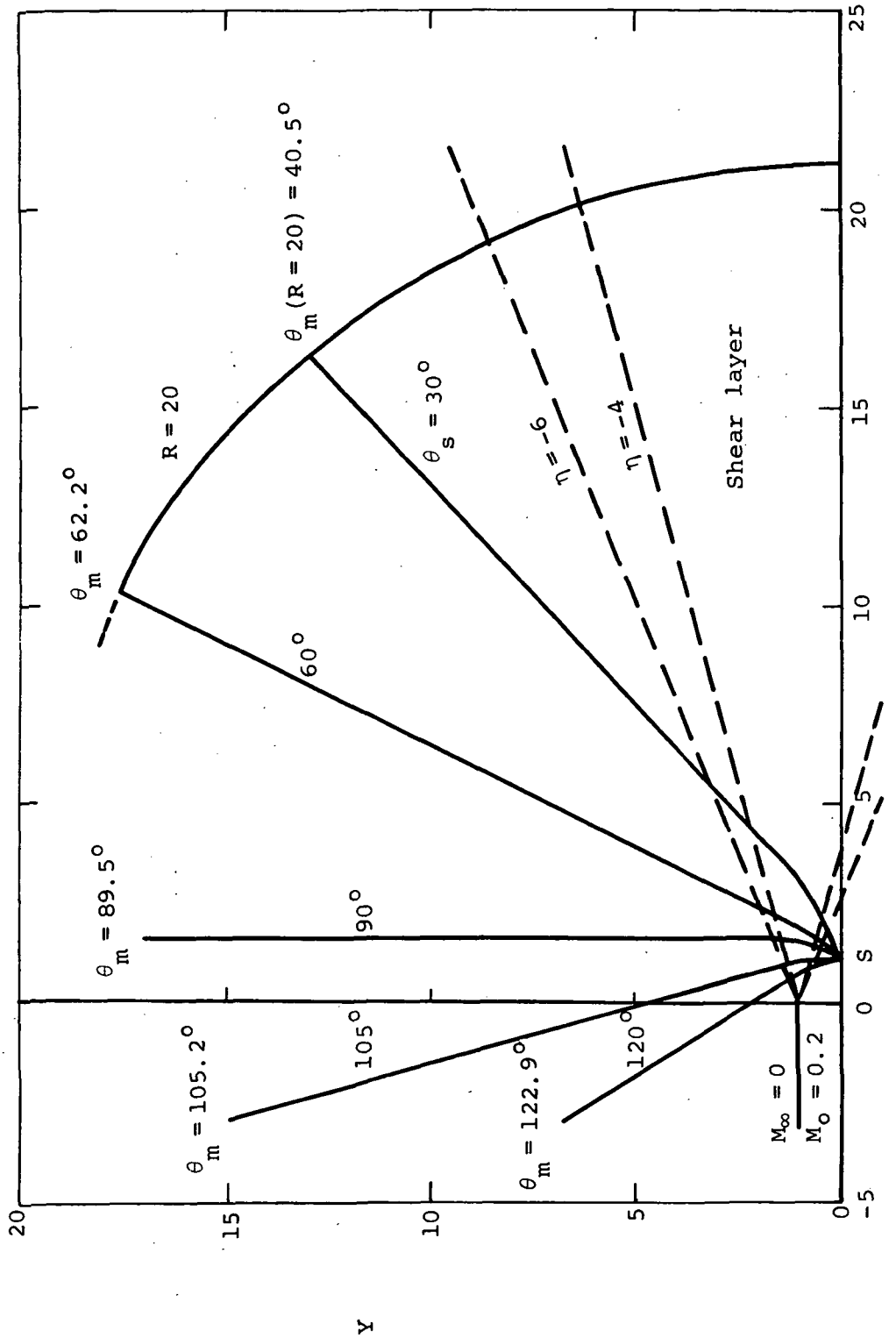

Figure 8.- Ray paths through shear layer; M_o = 0.2.

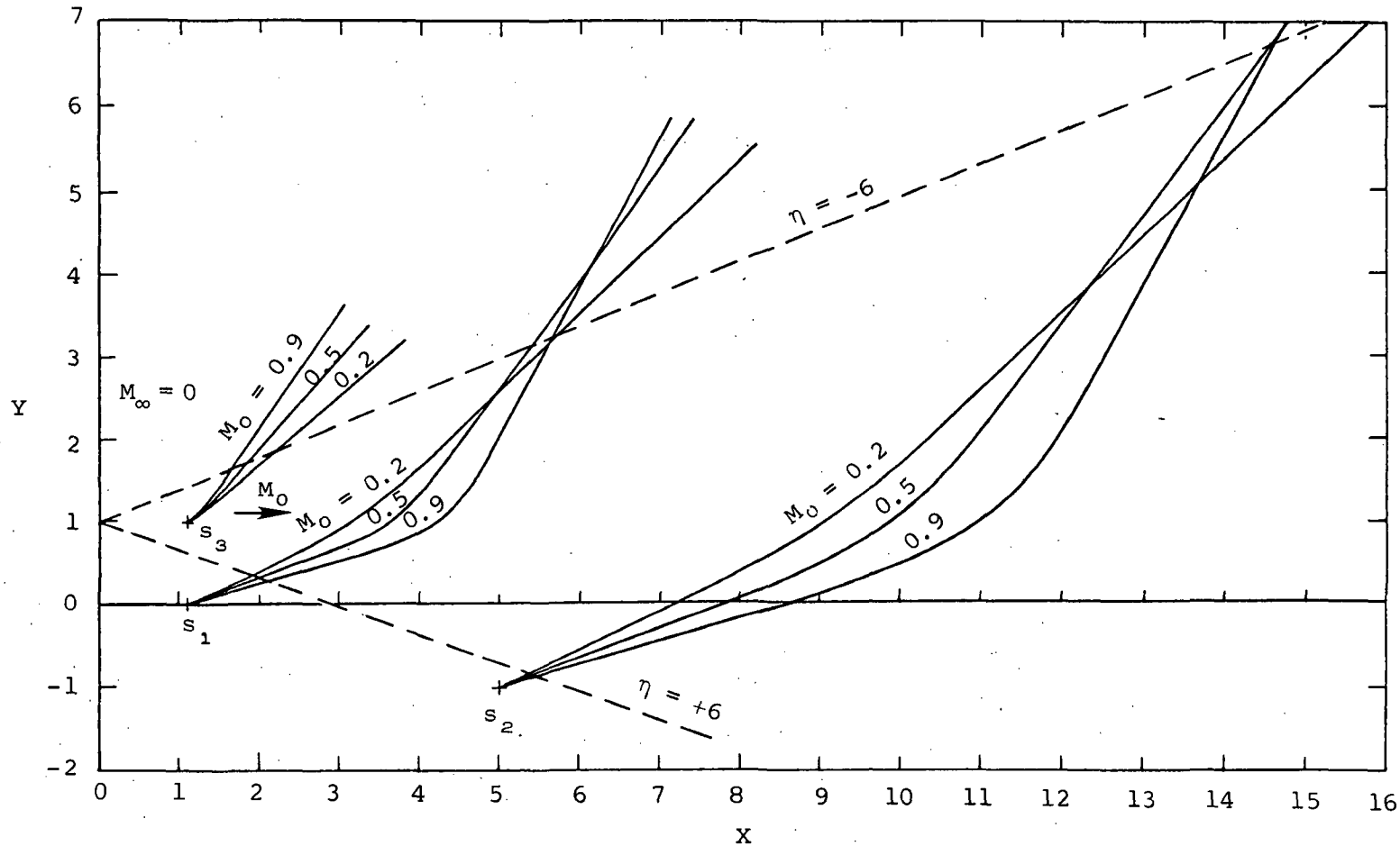

Figure 9.- Typical ray paths; $\theta_s = 30^o$.

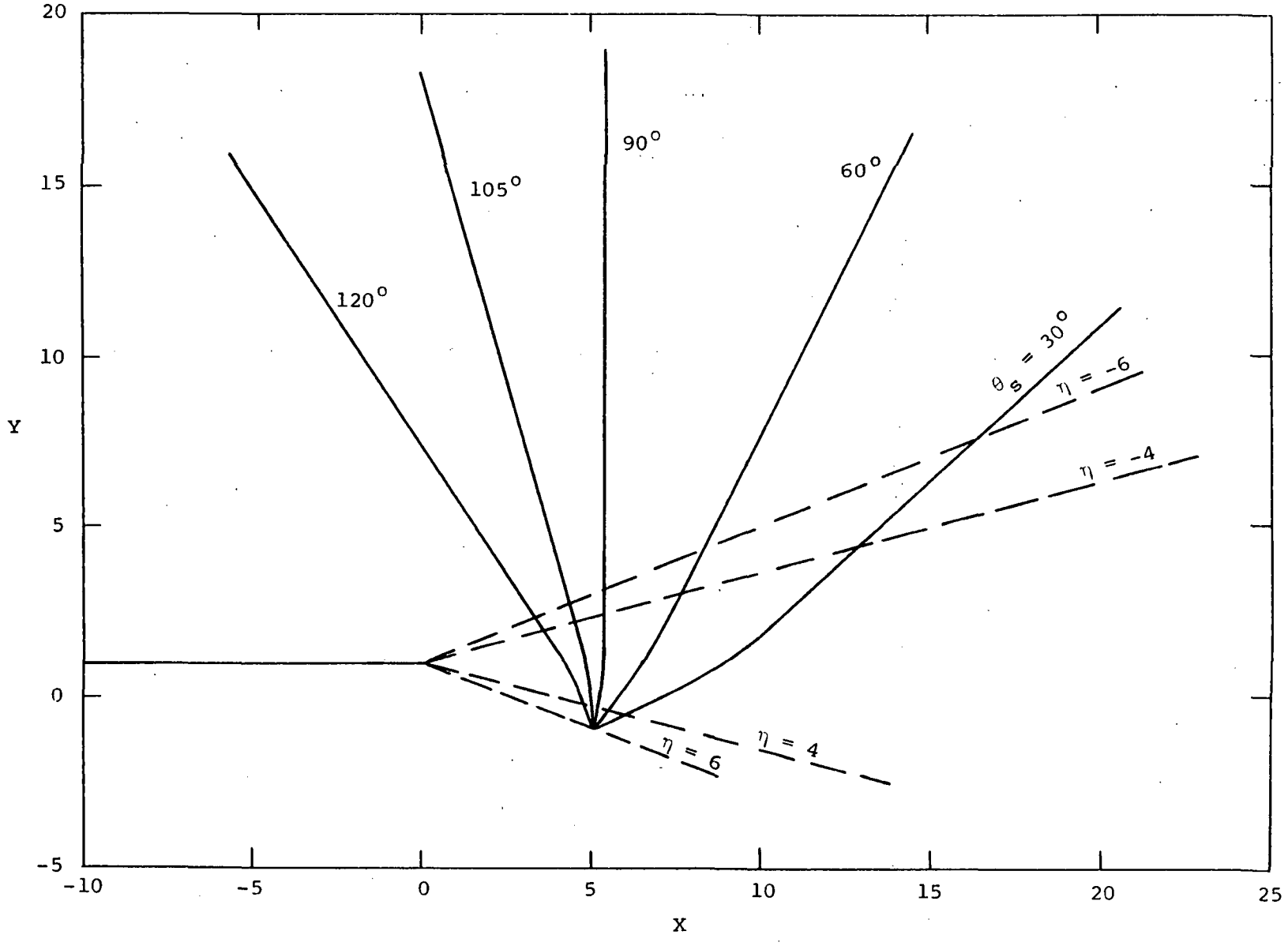

Figure 10.- Ray paths through shear layer for Source 2 of Figure 9; $M_0 = 0.2$.

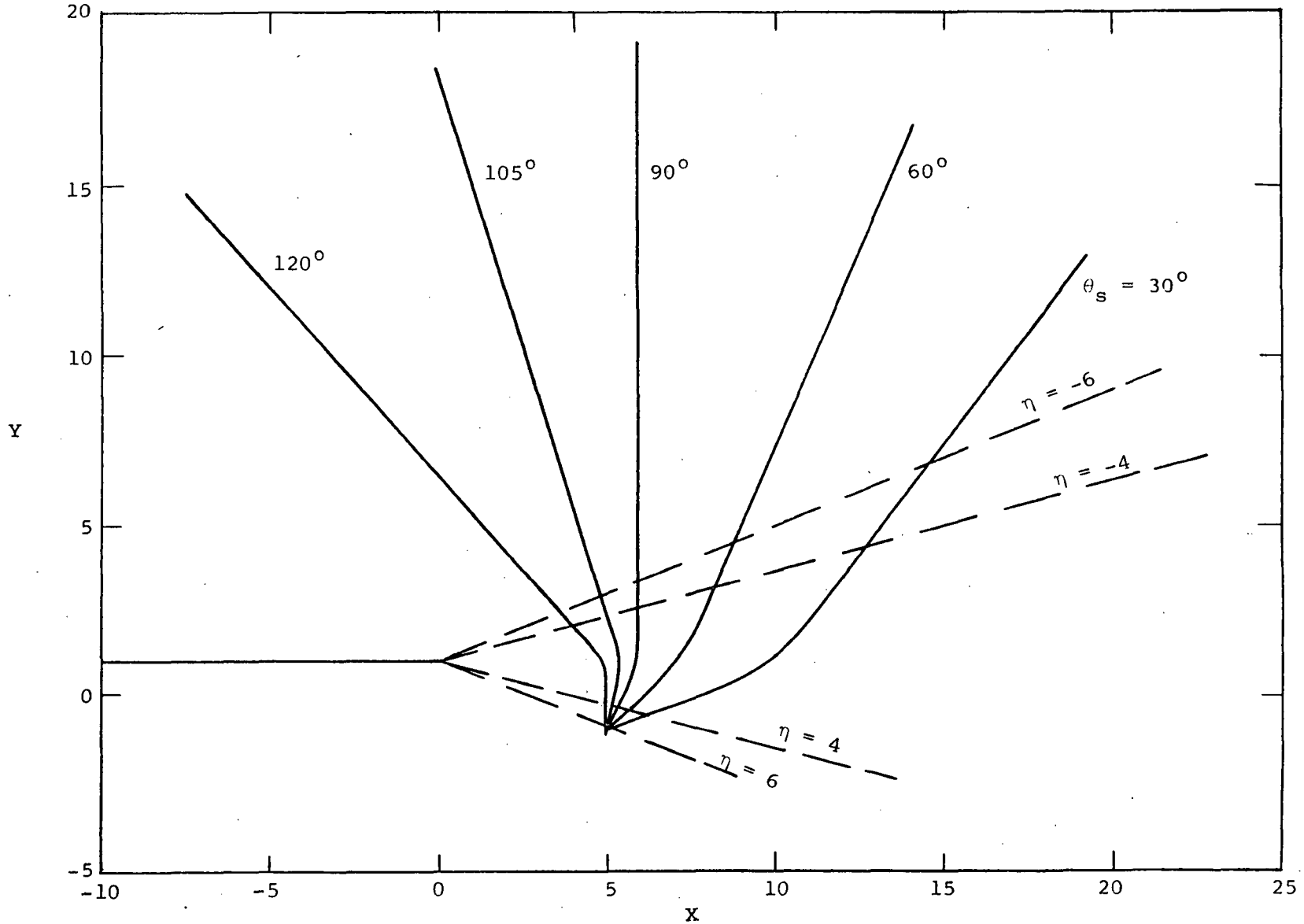

Figure 11.- Ray paths through shear layer for Source 2 of Figure 9; $M_o = 0.5$.

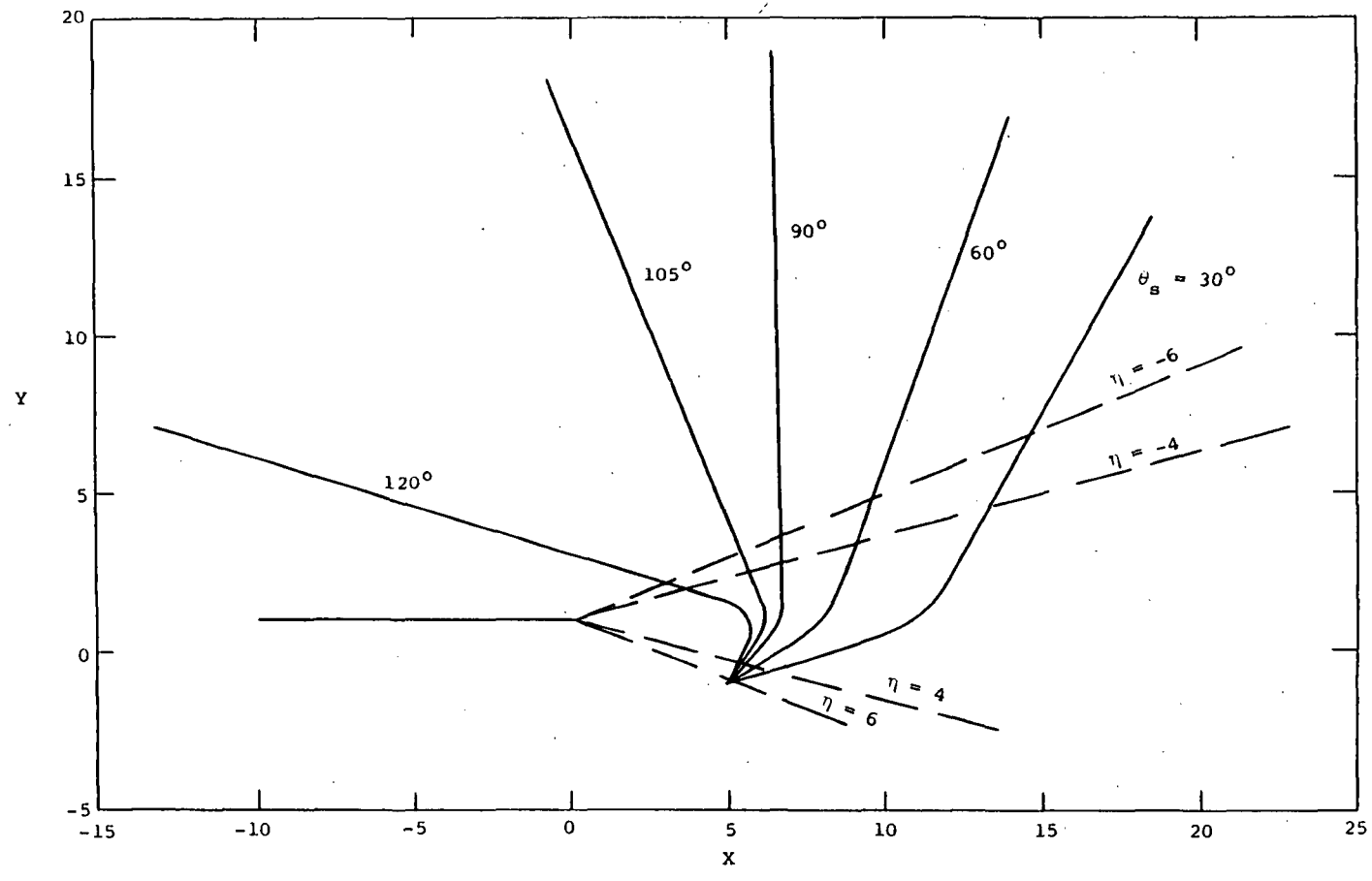

Figure 12.- Ray paths through shear layer for Source 2 of Figure 9; $M_0 = 0.9$.

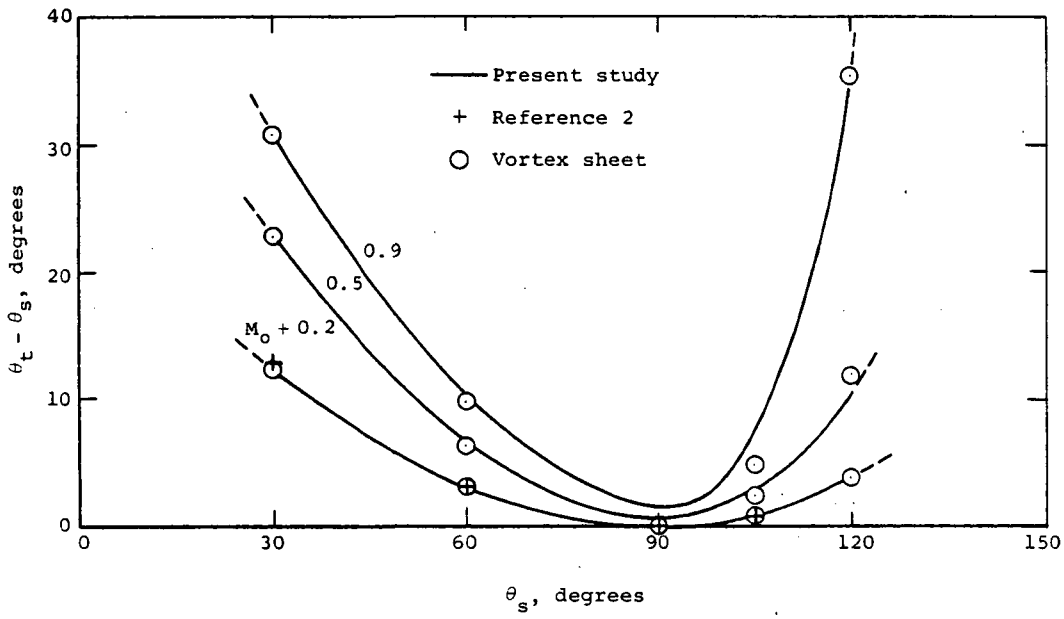

Figure 13.- Deflection of wavenormal by shear layer.

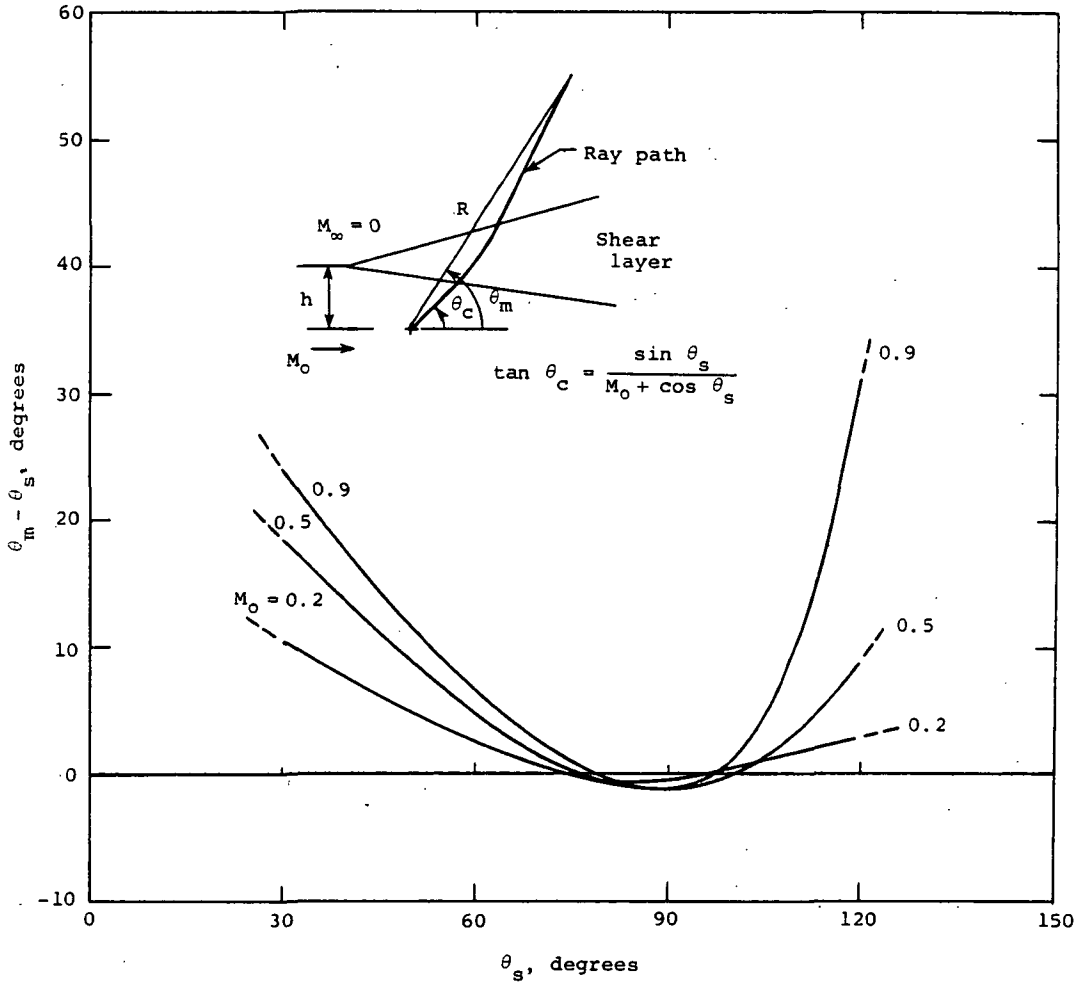

Figure 14.- Effective deflection of ray path by shear layer; h/R = 0.05.

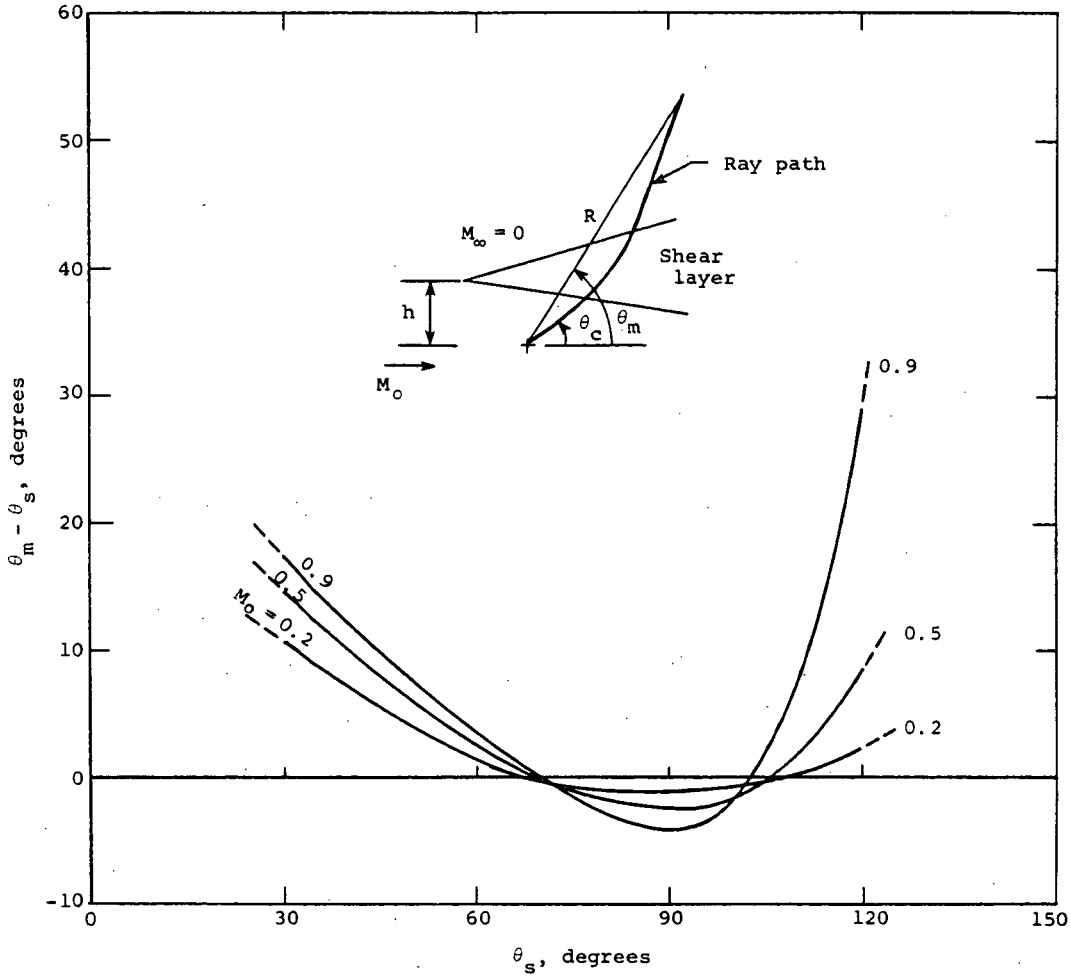

Figure 15.- Effective deflection of ray path by shear layer; h/R = 0.25.

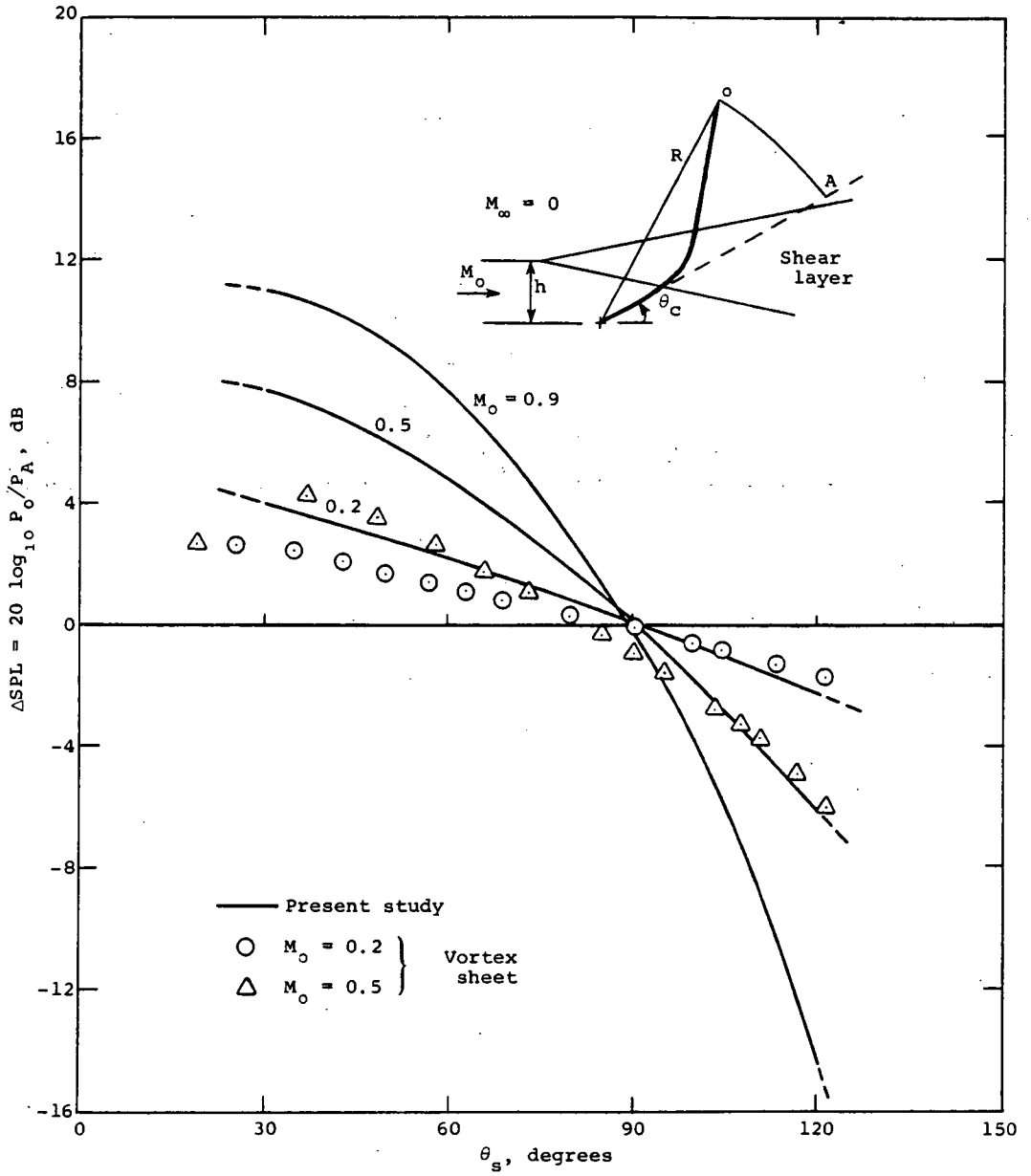

Figure 16.- Change in sound pressure from flow nonuniformity; h/R = 0.05.

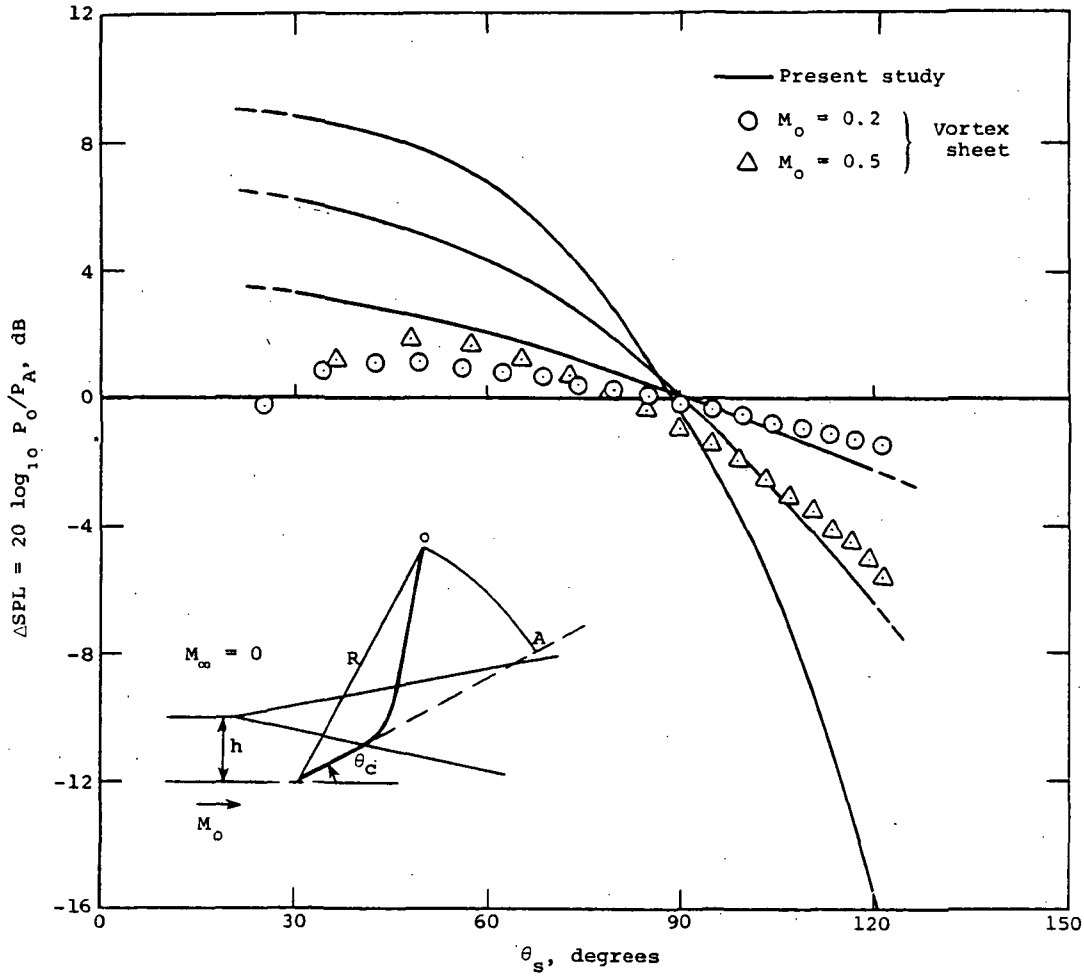

Figure 17.- Change in sound pressure from flow nonuniformity; h/R = 0.25.

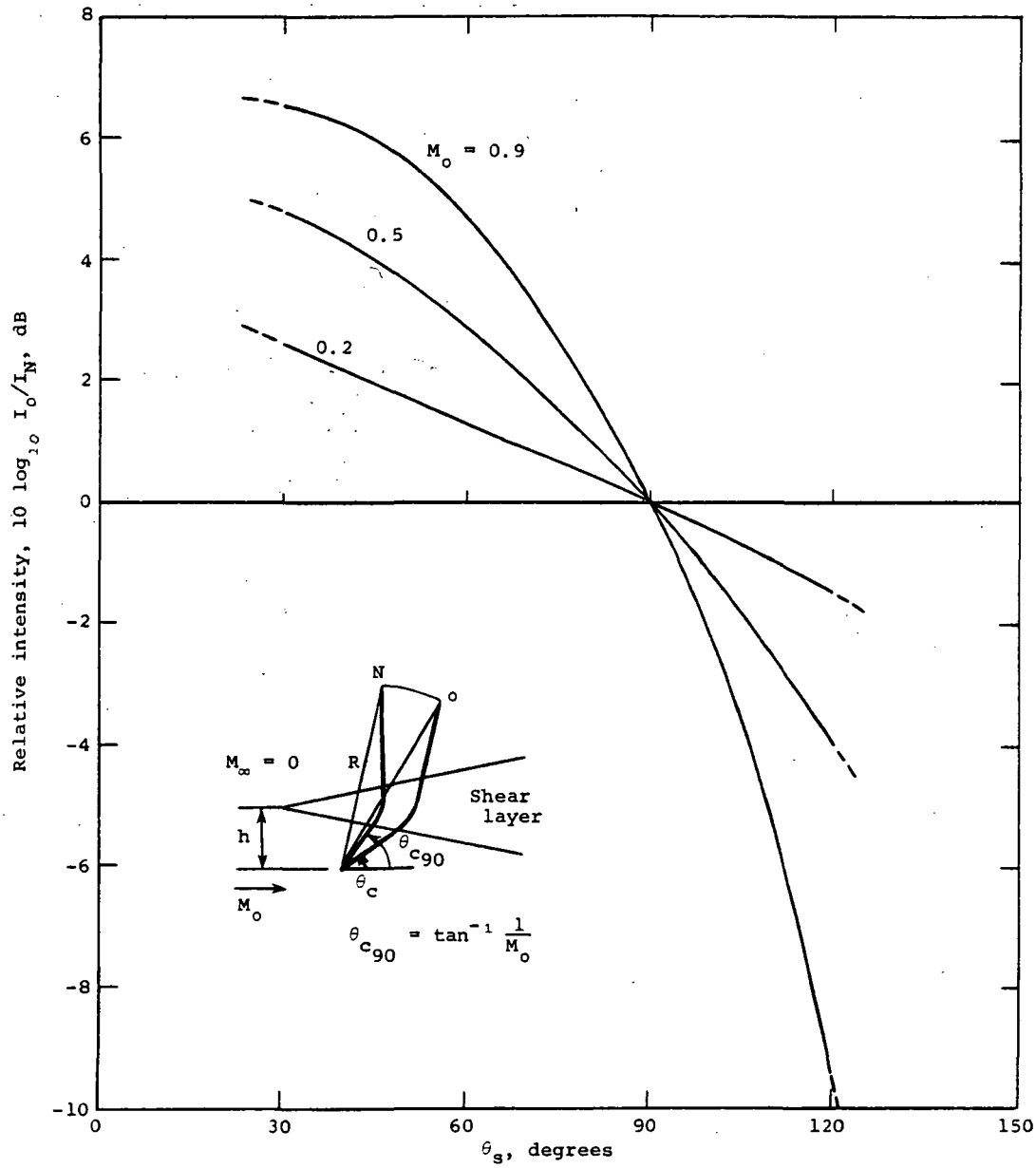

Figure 18.- Calculated relative intensity; h/R = 0.05.

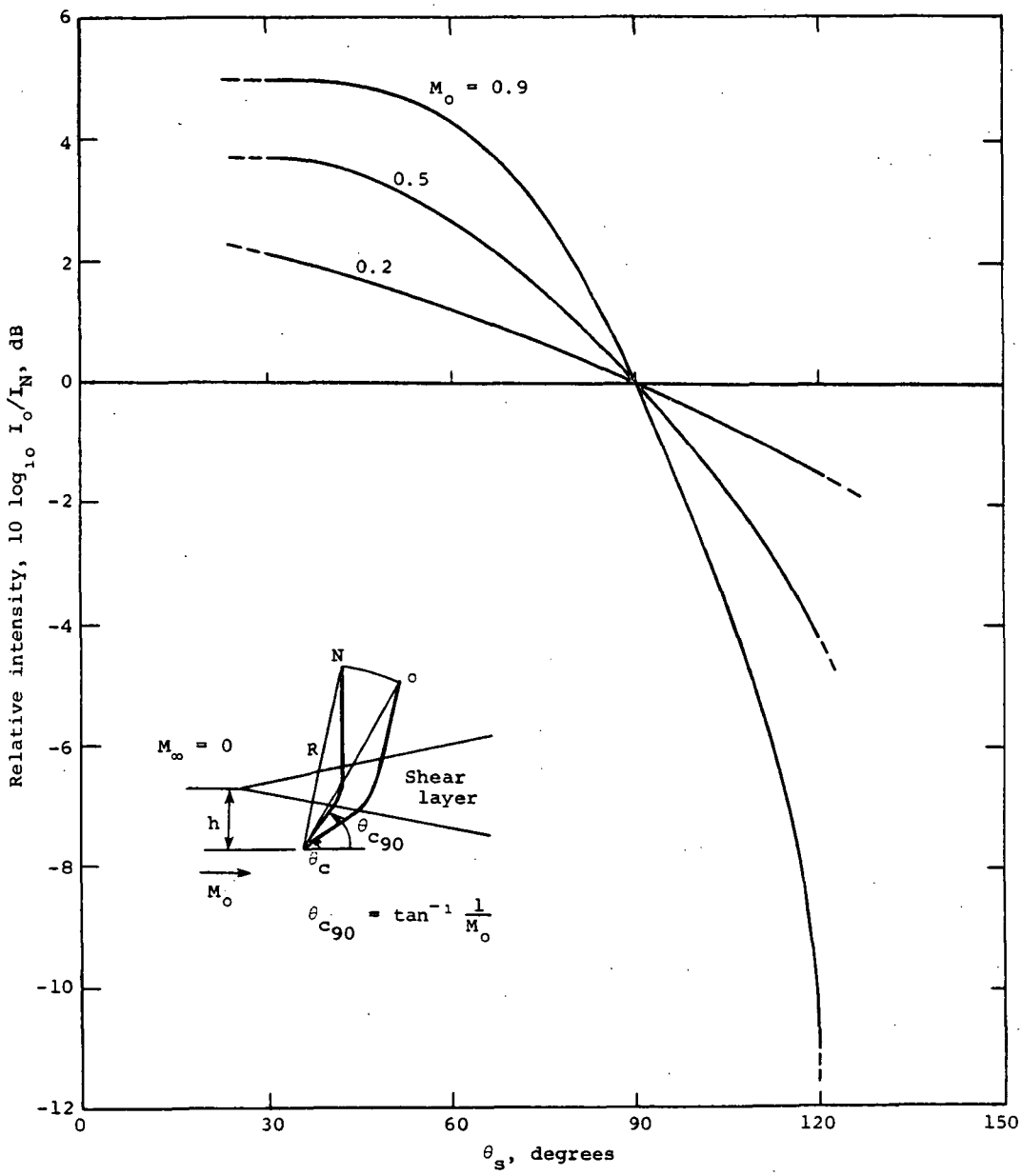

Figure 19.- Calculated relative intensity; h/R = 0.25.